



NOAA Pacific Marine Environmental Laboratory  
Ocean Climate Stations Project

## DATA ACQUISITION AND PROCESSING REPORT FOR KE017

<i>Site Name:</i>	Kuroshio Extension Observatory (KEO)
<b><i>Deployment Number:</i></b>	<b>KE017</b>
<i>Year Established:</i>	2004

<i>Nominal Location:</i>	32.3°N 144.6°E
<i>Anchor Position:</i>	32° 14.18'N 144° 34.89'E (est. watch circle, no triangulation)

<i>Deployment Date:</i>	September 26 <sup>th</sup> , 2019
<i>Recovery Date:</i>	July 20 <sup>th</sup> , 2020

<i>Project P.I.:</i>	Dr. Meghan F. Cronin
<i>Report Authors:</i>	N.D. Anderson, P. Berk, M.F. Cronin
<i>Data Processors:</i>	N.D. Anderson

<i>Date of Report:</i>	January 20, 2023
<i>Revision History:</i>	October 11, 2020

*Special Notes:* Weather constraints forced a single day deployment/recovery. The anchor drop was premature, and no CTDs or flybys were performed. Mooring went adrift 5/19/2020, and was later recovered by the Kaiyo Maru #1.

## Table of Contents

<b>1.0</b>	<b>Mooring Summary .....</b>	<b>1</b>
1.1	Mooring Description.....	2
1.2	Instrumentation on KE017 .....	5
<b>2.0</b>	<b>Data Acquisition .....</b>	<b>7</b>
2.1	Sampling Specifications .....	7
2.2	Data Returns .....	9
2.3	Known Sensor Issues .....	11
<b>3.0</b>	<b>Data Processing.....</b>	<b>13</b>
3.1	Buoy Positions.....	14
3.2	Meteorological Data.....	14
3.2.1	Winds.....	14
3.2.2	Air Temperature.....	15
3.2.3	Relative Humidity .....	15
3.2.4	Barometric Pressure.....	16
3.2.5	Rain .....	16
3.2.6	Shortwave Radiation.....	17
3.2.7	Longwave Radiation.....	18
3.3	Subsurface Data.....	20
3.3.1	Temperature .....	21
3.3.2	Pressure.....	21
3.3.3	Salinity.....	21
3.3.4	Deep SBE Data.....	24
3.3.5	Currents (Nortek Aquadopp).....	24
3.3.6	Acoustic Doppler Current Profiler (Aquadopp Profiler).....	26
<b>4.0</b>	<b>References .....</b>	<b>27</b>
<b>5.0</b>	<b>Acknowledgements.....</b>	<b>27</b>
<b>6.0</b>	<b>Contact Information .....</b>	<b>27</b>
	<b>APPENDIX A: Description of Data Quality Flags .....</b>	<b>28</b>
	<b>APPENDIX B: Primary Instrument High Resolution Data Plots .....</b>	<b>29</b>
	<b>APPENDIX C: Secondary Instrument High Resolution Data Plots.....</b>	<b>34</b>

## List of Tables

Table 1: Instruments deployed on KE017. ....	5
Table 2: Sampling parameters of the primary sensors on KE017. ....	8
Table 3: Sampling parameters for the secondary sensors on KE017. ....	8
Table 4: Recovery log displaying all instrument clock errors. ....	20

## List of Figures

Figure 1: KEO regional map, with the KE017 (2019) estimated position and JAMSTEC sediment trap .....	1
Figure 2: KE017 as deployed .....	3
Figure 3: KE017 mooring diagram.....	4
Figure 4: Buoy diagram showing bridle arrangement.....	6
Figure 5: KE017 battery swap diagram and acquisition system battery voltage .....	12
Figure 6: High-resolution wind measurements on KE017.....	14
Figure 7: High-resolution air temperature measurements on KE017 .....	15
Figure 8: High-resolution relative humidity measurements on KE017 .....	15
Figure 9: High-resolution barometric pressure data from KE017 .....	16
Figure 10: Raw KE017 radiometer data .....	17
Figure 11: Downwelling LWR (pre-QC) showing spikes, but also data drift.....	18
Figure 12: Net longwave radiation (pre-QC) on KE017 .....	19
Figure 13: Difference plot of raw (pre-QC) downwelling LWR.....	19
Figure 14: High-resolution subsurface pressure data on KE017 .....	21
Figure 15: KE017 buoy velocities used to correct currents.....	25

## Data Acquisition and Processing Report for OCS Mooring KE017

### 1.0 Mooring Summary

The NOAA Ocean Climate Stations reference mooring at the Kuroshio Extension Observatory (KEO) site was established with the deployment of the KE001 mooring in June 2004. The 2004 deployment was part of the first year of the two-year Kuroshio Extension System Study (KESS). At the conclusion of KESS, a partnership with the Japan Agency for Marine-Earth Science and Technology (JAMSTEC) was formed.

#### Operational KEO Map

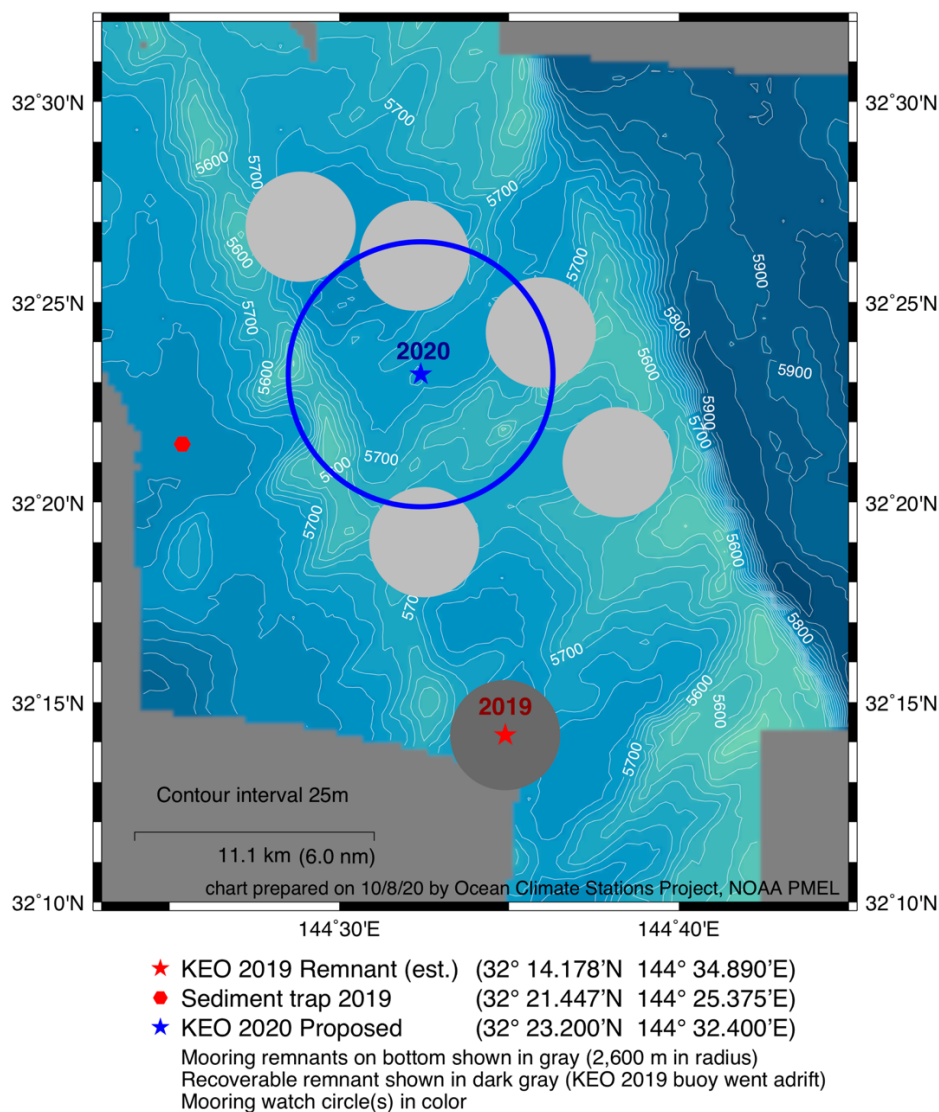


**Figure 1: KEO regional map, with the KE017 (2019) estimated position (anchor dropped with no triangulation, location estimated from watch circle) and JAMSTEC sediment trap.**



KE017 was the 16<sup>th</sup> deployment at the KEO site (the KE004 name was given to a buoy deployed at the nearby JKEO site, maintained by JAMSTEC). The mooring was deployed on September 26<sup>th</sup>, 2019 by the M/V KAIYO MARU #1. The surface buoy, having gone adrift May 19<sup>th</sup>, 2020, was recovered by the same ship on July 20<sup>th</sup>, 2020. The captain and crew of the ship are gratefully acknowledged for their support in maintaining this long-term reference station. Special recognition is extended to the entire team aboard the KAIYO MARU #1 for performing the recovery operations without OCS personnel aboard due to COVID-19 travel restrictions.

Several typhoons affected the KE017 mooring. After delaying deployment, Typhoon Tapah (September 17 – 22, 2019) left a narrow weather window behind it, forcing deployment (KE017) and recovery (KE016) operations into a single day. No CTD cast or buoy flyby was performed, and the anchor was dropped slightly early to preserve time for recovery operations. Typhoon Hagibis, initially a category 5 super typhoon, passed KEO to the west, making landfall in Japan as a category 2 equivalent storm on October 12, 2019. Typhoon Bualoi passed within 75 nm of the KEO mooring on October 24, 2019, and a maximum realtime wind gust of 30.7 m/s (~ 70 mph) was recorded.

## 1.1 Mooring Description

The KE017 mooring was a slack-line mooring, with a nominal scope of 1.4. Non-rotating 7/16" (1.11cm) diameter wire rope, jacketed to 1/2" (1.27cm), was used in the upper 700m of the mooring line. Plastic fairings were installed on the wire rope from 1m – 150m and 240m – 350m. The remainder of the mooring line consisted of plaited 8-strand nylon line, spliced to buoyant polyolefin, as shown in Figure 3. There were 18 glass balls in line above the acoustic release. The 8,240lb (3,738kg) anchor was fabricated from scrap railroad wheels.

The upper portion of the mooring was kept fairly vertical by using a reverse catenary design, but less so than with taut-line moorings. Since instrument depths change on a slack line mooring, most KEO instruments measure pressure. Interpolated pressures are used in salinity calculations where no pressure measurements exist.

The surface buoy was a 2.6m fiberglass-over-foam discus buoy, with a central instrument well. It had an aluminum tower and a stainless steel bridle.

OCS partner groups also provided mooring instrumentation. The PMEL Carbon Group (PI: Dr. Adrienne Sutton) contributed an SBE16 package (with an attached oxygen sensor and fluorometer) and a Sami pH sensor mounted on the buoy bridle, along with their primary CO<sub>2</sub> flux monitoring system housed in the buoy well.

Four JAMSTEC backscatter meters (PI: Dr. Makio Honda) were added to the KE017 mooring and, for the first time, an underwater camera. Although featured on previous KEO moorings (and provided by Dr. Jie Yang of the University of Washington Applied Physics Lab), no Passive Acoustic Listening (PAL) device was deployed in 2019. OCS is not

responsible for the acquisition or processing of partner data, so no further discussion of these systems are included in this report. All OCS and partner systems with corresponding instrumentation are shown in the mooring diagram (Figure 3).



Figure 2: KE017 as deployed.

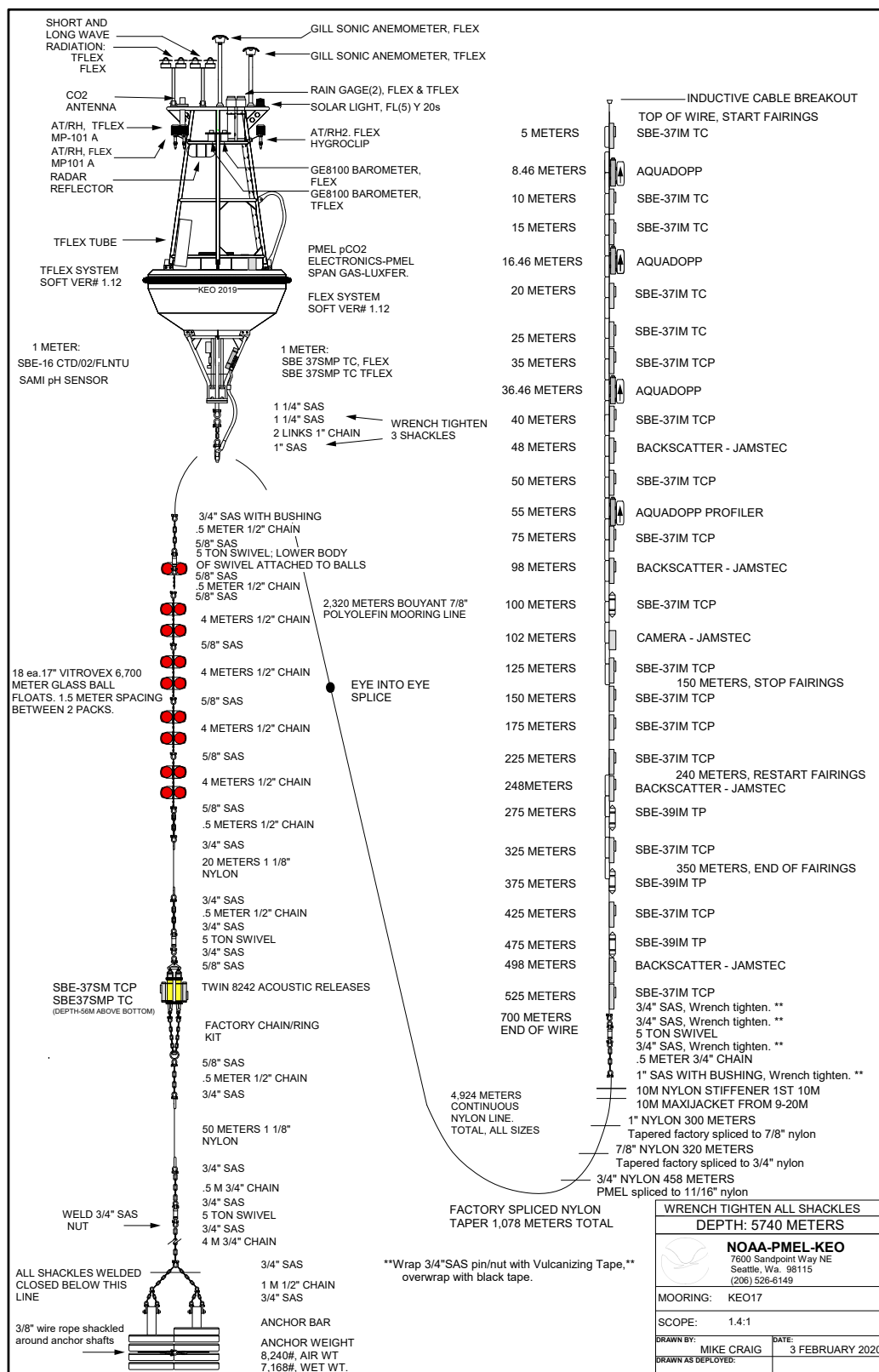


Figure 3: KE017 mooring diagram.

## 1.2 Instrumentation on KE017

The following instrumentation was deployed on KE017. Redundant data acquisition systems were used, Flex and TFlex. Flex meteorological sensors are generally considered primary. Any substitutions are noted in the relevant section of this report.

Deployment:		KE017			
Met Sensors		Model	Serial #		Notes
Height	Acquisition	FLEX			
2.6m	ATRH	Rotronics MP-101A	104889		
2.6m	ATRH2	Rotronics HygroClip	20218252		
4.2m	Wind	Gill	14180060		
2.5m	BP	GE8100	10879093		
3.1m	Rain	RM Young	745		
3.6m	SWR	Eppley PSP	38484		
3.6m	LWR	Eppley PIR	38693		
	Acquisition	TFLEX	2006		
2.6m	ATRH	Rotronics MP-101A	91589		
3.8m	Wind	Gill	11520107		
2.5m	BP	GE8100	10975354		
3.1m	Rain	RM Young	1950		
3.6m	SWR	Eppley PSP	38428		
3.6m	LWR	Eppley PIR	38439		
	CO2	Electronics	PMEL	146	
		Span Gas	Luxfer	JJ13178	
Subsurface Instrumentation					
Bridge		Model	Serial #		Notes
1m	SST/C	SBE37SMP - TC	11554		Flex, AA
1m	SST/C	SBE37SMP - TC	7089		TFLEX
1m	pH	Sami	59U		CO2
1m	SST/C	SBE16+V2	50164		CO2
1m	Oxygen	Optode	1725		Attached to CO2 SBE16+
1m	Fluorescence	ECO FLNTUS	3339		Attached to CO2 SBE16+
Depth		Model	Serial #	IM ID	Notes
5m	TC	SBE37IM - TC	20433	01	
8.46m	ADCM	AquaDopp	8473	02	
10m	TC	SBE37IM - TC	6077	03	
15m	TC	SBE37IM - TC	6078	04	
16.46m	ADCM	AquaDopp	5952	05	
20m	TC	SBE37IM - TC	6140	06	
25m	TC	SBE37IM - TC	6079	07	
35m	TCP	SBE37IM - TCP	16293	08	
36.46m	ADCM	AquaDopp	9980	09	
40m	TCP	SBE37IM - TCP	7096	10	
48m		JAMSTEC Backscatter			
50m	TCP	SBE37IM - TCP	12519	11	
55m	ADCP	Aquadopp Profiler	13314		
75m	TCP	SBE37IM - TCP	7785	12	
98m		JAMSTEC Backscatter	5175		
100m	TCP	SBE37IM - TCP	7102	13	
102m		Jamstec Camera			
125m	TCP	SBE37IM - TCP	7100	14	
150m	TCP	SBE37IM - TCP	7099	15	
175m	TCP	SBE37IM - TCP	7098	16	
225m	TCP	SBE37IM - TCP	7097	17	
248m		JAMSTEC Backscatter	BB1741		
275m	TP	SBE39IM - TP	4361	18	
325m	TCP	SBE37IM - TCP	7095	19	
375m	TP	SBE39IM - TP	4359	20	
425m	TCP	SBE37IM - TCP	7094	21	
475m	TP	SBE39IM - TP	4358	22	
498m		JAMSTEC Backscatter	TR905		
525m	TCP	SBE37IM - TCP	7093	23	
700m	End of Wire				
Release	TCP	SBE37SM - TCP	10504		non pumped w/ pressure
Release	TCP	SBE37SMP - TC	3802		pumped, no pressure

**Table 1: Instruments deployed on KE017.**

Since 2007, the measurement point for bridle sensors, including the SST/C, is known to have varied between 1.0 - 1.3m depth. Uncertainties in actual measurement depth are introduced by changes in buoy waterlines, variation between instrument mounting locations, and alteration of measurement points with different instrument versions. For these reasons, the nominal depth for all bridle sensors is stated as 1m.

Due to the SSTC versions used on KE017, the thermistors ended up at the same depth (1.26m). However, the conductivity cell positions differed slightly as noted in the buoy diagram below. KE017 was the first KEO buoy to have replaced both older Druck barometers with GE8100 TERPS barometers.

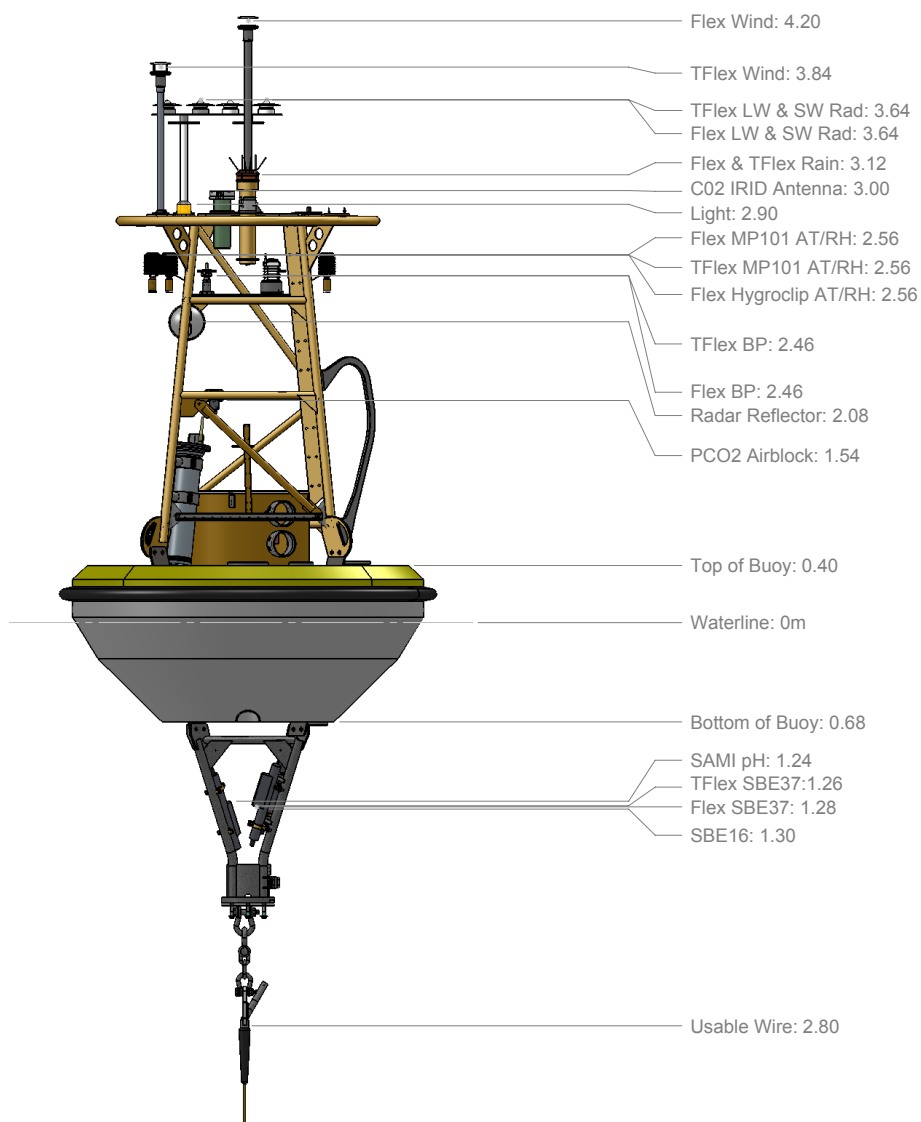


Figure 4: Buoy diagram showing bridle arrangement. The SBE16 package contains a suite of sensors.

## 2.0 Data Acquisition

Two independent data acquisition systems were deployed on KE017, Flex and TFlex. Both systems telemetered hourly averaged surface data via Iridium satellite, with Flex also transmitting hourly data from the subsurface instruments. High-resolution data are logged internally throughout the deployment in subsurface instruments, and downloaded upon recovery of the mooring. KE017 was the sixth KEO mooring to have phased out the ATLAS system and implemented the newer TFlex.

Position information associated with real-time data comes through the Iridium satellite network. Buoy latitude and longitude are transmitted to shore via three GPS devices on the Flex, TFlex, and CO<sub>2</sub> systems. The Flex GPS measurements are hourly and TFlex GPS measurements occur every six hours. Occasional position errors were spotted and removed during quality control operations.

The KEO mooring site is nominally at 32.3°N, 144.6°E. The actual anchor position is different for each deployment, and the slack line mooring has a watch circle radius greater than 5km. For users performing intercomparisons, it may be important to use the actual position of the buoy from the GPS data. Also, depths of the subsurface measurements will change over time on the slack mooring. Depths shown in the delivered KEO files represent the nominal location of the sensor on the mooring line. To determine the true depth of the measurement, use the accompanying pressure time series data.

### 2.1 Sampling Specifications

The following tables describe the high-resolution sampling schemes for the KE017 mooring, for both the primary and secondary systems. Observation times in data files are assigned to the center of the averaging interval. The Flex system sensors are usually considered primary, and the reasoning behind any substitutions are described in the relevant sections that follow.



**PRIMARY SENSORS**

Measurement	Sample Rate	Sample Period	Sample Times	Recorded Resolution	Acquisition System
Wind Speed/Direction	2 Hz	2 min	2359-0001, 0009-0011...	10 min	FLEX
Air Temperature + Relative Humidity	1 Hz	2 min	2359-0001, 0009-0011...	10 min	FLEX
Barometric Pressure	1 Hz	2 min	2359-0001, 0009-0011...	10 min	TFLEX
Rain Rate	1 Hz	1 min	0000-0001, 0001-0002...	1 min	FLEX
Shortwave Radiation	1 Hz	1 min	0000-0001, 0001-0002...	1 min	FLEX
Longwave Radiation (Thermopile, Case & Dome Temperatures)	1 Hz	1 min	0000-0001, 0001-0002...	1 min	TFLEX
Seawater Temperature, Pressure & Conductivity	1 per 10 min	Instant.	0000, 0010,...	10 min	Internal
Ocean Currents (Point)	1 Hz	2 min	2359-0001, 0009-0011...	10 min	Internal
Ocean Currents (Profile)	1 Hz	2 min	0029-0031, 0059-0101...	30 min*	Internal
GPS Position	1 per hr	Instant.	0000, 0100, ...	1 hr	FLEX

Table 2: Sampling parameters of the primary sensors on KE017.

\* Newly updated this year from hourly to 30 min.

**SECONDARY SENSORS**

Measurement	Sample Rate	Sample Period	Sample Times	Recorded Resolution	Acquisition System
Wind Speed/Direction	2 Hz	2 min	2359-0001, 0009-0011...	10 min	TFLEX
Air Temperature + Relative Humidity	1 Hz	2 min	2359-0001, 0009-0011...	10 min	TFLEX
Barometric Pressure	1 Hz	2 min	2359-0001, 0009-0011...	10 min	FLEX
Rain Rate	1 Hz	1 min	0000-0001, 0001-0002...	1 min	TFLEX
Shortwave Radiation	1 Hz	1 min	0000-0001, 0001-0002...	1 min	TFLEX
Longwave Radiation (Thermopile, Case & Dome Temperatures)	1 Hz	1 min	0000-0001, 0001-0002...	1 min	FLEX
SSTC	1 per 10 min	Instant.	0000, 0010,...	10 min	Internal
GPS Position	1 per 6 hrs	Instant.	0000, 0600, ...	6 hr	TFLEX

Table 3: Sampling parameters for the secondary sensors on KE017.

## 2.2 Data Returns

Data returns are calculated from the highest-resolution data, comparing the number of records available to the total amount of records expected for the period. The following list shows the data returns from the surface and subsurface measurements from both acquisition systems.

### Flex 0002:

#### Data Return Summary

2019-09-26 05:15:00 to 2020-05-19 03:00:00

Sensor	Deployed	Obs	Return
=====			
AT1	33971	33943	99.9%
AT2	33971	33943	99.9%
RH1	33971	33943	99.9%
RH2	33971	33943	99.9%
WIND1	33971	33943	99.9%
BP1	33971	33943	99.9%
RAIN1	339707	337508	99.4%
SWR1	339707	337560	99.4%
LWR1	339707	337609	99.4%

#### Subsurface Temperature Profile

1m	33971	33971	100.0%	
5m	33971	33971	100.0%	
10m	33971	33971	100.0%	
15m	33971	33971	100.0%	
20m	33971	0	0.0%	* Some realtime available
25m	33971	11384	33.5%	
35m	33971	33971	100.0%	
40m	33971	33971	100.0%	
50m	33971	33971	100.0%	
75m	33971	33971	100.0%	
100m	33971	33971	100.0%	
125m	33971	33971	100.0%	
150m	33971	33971	100.0%	
175m	33971	33971	100.0%	
225m	33971	33971	100.0%	
275m	33971	33098	97.4%	
325m	33971	33971	100.0%	
375m	33971	33971	100.0%	
425m	33971	33971	100.0%	
475m	33971	0	0.0%	* Some realtime available
525m	33971	33971	100.0%	

#### Subsurface Pressure Profile

35m	33971	33971	100.0%
40m	33971	33971	100.0%
50m	33971	33971	100.0%
75m	33971	33971	100.0%
100m	33971	33971	100.0%



125m	33971	33971	100.0%
150m	33971	33971	100.0%
175m	33971	33971	100.0%
225m	33971	33971	100.0%
275m	33971	33098	97.4%
325m	33971	33971	100.0%
375m	33971	33971	100.0%
425m	33971	33971	100.0%
475m	33971	0	0.0%
525m	33971	33971	100.0%

## Subsurface Salinity Profile

1m	33971	33971	100.0%
5m	33971	33971	100.0%
10m	33971	33971	100.0%
15m	33971	33971	100.0%
20m	33971	0	0.0%
25m	33971	11384	33.5%
35m	33971	33971	100.0%
40m	33971	33971	100.0%
50m	33971	33971	100.0%
75m	33971	33971	100.0%
100m	33971	33971	100.0%
125m	33971	33971	100.0%
150m	33971	33971	100.0%
175m	33971	33971	100.0%
225m	33971	33971	100.0%
325m	33971	33971	100.0%
425m	33971	33971	100.0%
525m	33971	33971	100.0%

## AQD Current Velocity

8m	33971	33971	100.0%	* Some realtime available
16m	33971	0	0.0%	
36m	33971	33971	100.0%	

**TFlex 2006:**

## Data Return Summary

2019-09-26 05:15:00 to 2020-05-19 03:00:00

Sensor	Deployed	Obs	Return
=====			
AT1	33971	33971	100.0%
RH1	33971	33971	100.0%
WIND1	33971	3183	9.4%
BP1	33971	33971	100.0%
RAIN1	339707	155135	45.7%
SWR1	339707	45067	13.3%
LWR1	339707	338541	99.7%
SST1	33971	33971	100.0%
SSC1	33971	33971	100.0%
SSS1	33971	18400	54.2%

## 2.3 Known Sensor Issues

Surface sensors displayed average performance during KE017. Minor issues with calibration, drift, or offsets are addressed in the instrument-specific subsections within the discussion of meteorological data (Section 3.2). Though a few failures occurred, redundancy of the surface meteorological measurements resulted in high effective surface data returns.

Subsurface sensors had several issues during and after the KE017 deployment. The Flex SSTC was selected as the primary SSTC due to its lower variability and fewer spikes when compared to the TFlex SSTC. The 5m SBE had a bad post-cal, performed after replatinization of the conductivity cell, so the post-cal did not represent the recovered state of the instrument. The 5m data are distributed with the precal applied, with additional corrections based on density comparisons against surrounding sensors.

The 20m and 475m sensors did not download upon recovery (due to a broken battery terminal and a corrupt data record, respectively), so hourly realtime data were included in the distributed records as the highest resolution data available at those depths.

Records from 25m and 275m ended early due to dead batteries, with 11k and 33k records, respectively, out of a total potential of 56k timestamps (34k timestamps if considering only the moored period). A missing post-calibration for the 225m instrument was discovered during data processing, but was located by Seabird Inc. and utilized in data processing.

Curiously, the 425m pressure record (in both delayed-mode and realtime data) moved inversely to pressure data from surrounding instruments throughout KE017. The issue was found to be an erroneous 2019 calibration that the manufacturer had loaded into the instrument prior to deployment, so the bad calibration was unapplied, and the data were distributed with the 2021 post-cruise calibration applied instead. A calibration from 2017 was briefly considered for use, but was not selected because 1) an entire deployment (KE015) had passed since the 2017 calibration, 2) the manufacturer noted the instrument had been modified in 2019, and 3) the post-cruise calibration more closely represented the state of the instrument during KE017 and was deemed more trustworthy (although the average pressure difference between the 2017 and 2021 calibrations was just  $\sim 0.075$  dbar). Two additional 2019 calibrations for this instrument were found in the database, but both were performed prior to modification (one of which was the valid post-calibration for KE015, but neither represented the state of the instrument as deployed on KE017).

A single Aquadopp current meter (S/N 5952) did not download. No delayed-mode data were recovered from this instrument, but realtime hourly data were distributed alongside the delayed-mode data from other depths.

Apart from individual sensor issues, one of the two primary batteries that power the Flex system was dead when technicians arrived at the Japanese port of Kurihama. Both batteries passed pre-cruise checks, but one was miswired in manufacturing. After the 2 batteries were connected for shipment via a “Y” cable, the batteries shorted en route to Japan, draining the properly wired battery and melting internal plastic components on the other. Technicians were able to salvage the miswired battery, which was re-wired in tandem with a large battery scavenged from the TFlex to power the Flex system. A battery from the spare TFlex was utilized to help power the primary TFlex at a slightly reduced voltage. This setup provided 100% power to the Flex system, and ~80% power to the TFlex. Priority was given to the Flex system because it drives communication with the inductive instruments and allows the acquisition of realtime subsurface data. Battery sizes (large/medium), charge status (red/green), and the rearrangement to optimize power for the Flex system is depicted below.

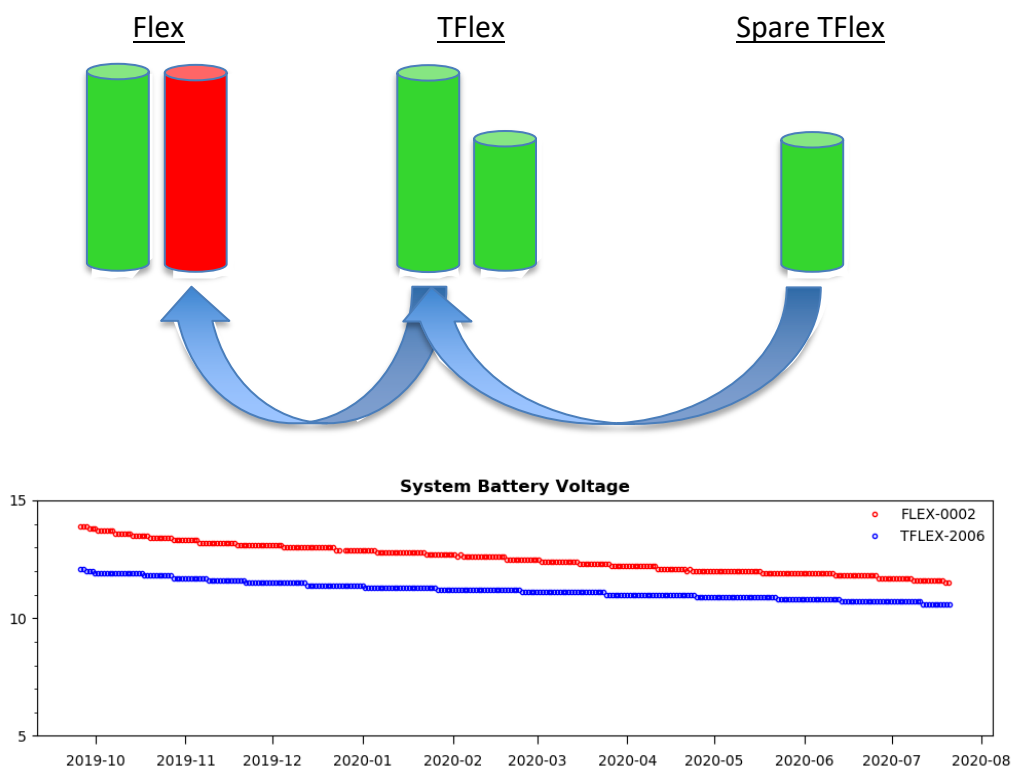


Figure 5: KE017 battery swap diagram (top) and acquisition system battery voltage (bottom).

### 3.0 Data Processing

Processing of data from OCS moorings is performed after the data are returned to PMEL. There are some differences between OCS data and data from GTMBA moorings, but standard methods described below are applied whenever possible. The process includes assignment of quality flags for each observation, which are described in Appendix A. Any issues or deviations from standard methods are noted in processing logs and in this report.

Raw data recovered from the internal memory of the data acquisition system are first processed using computer programs. Instrumentation recovered in working condition is returned to PMEL for post-recovery calibration before being reused on future deployments. These post-recovery calibration coefficients are compared to the pre-deployment coefficients. If the comparison indicates a drift larger than the expected instrument accuracy, the quality flag is lowered for the measurement. If post-recovery calibrations indicate that sensor drift was within expected limits, the quality flag is raised. Post-recovery calibrations are not generally applied to the data, except for seawater salinity, or as otherwise noted in this report. Failed post-recovery calibrations are noted, along with mode of failure, and quality flags are left unchanged to indicate that pre-deployment calibrations were applied and sensor drift was not estimated.

The automated programs also search for missing data, and perform gross error checks for data that fall outside physically realistic ranges. A computer log of potential data problems is automatically generated as a result of these procedures.

Time series plots, difference plots, and comparison plots are generated for all data. Plots of differences between adjacent subsurface temperature measurements are also generated. Statistics, including the mean, median, standard deviation, variance, minimum and maximum are calculated for each time series.

Trained analysts examine individual time series and statistical summaries. Data that have passed gross error checks, but which are unusual relative to neighboring data in the time series, or which are statistical outliers, are examined on a case-by-case basis. Mooring deployment and recovery logs are searched for corroborating information such as battery failures, vandalism, damaged sensors, or incorrect clocks. Consistency with other variables is also checked. Data points that are ultimately judged to be erroneous are flagged, and in some cases, values are replaced with “out of range” markers. For a full description of quality flags, refer to Appendix A.

For some variables, additional post-processing after recovery is required to ensure maximum quality. These variable-specific procedures are described below.

### 3.1 Buoy Positions

Since KEO is a slack-line mooring with a long scope, the buoy has a watch circle radius of more than 5km. When using KEO data in scientific analyses, it may be appropriate to consider the actual GPS position of the buoy rather than its nominal position. Gross error checking was performed to eliminate values outside the watch circle, but no further processing was performed, and positions inside the watch circle were used to determine buoy velocities for processing ocean current data.

### 3.2 Meteorological Data

All primary meteorological sensors on KE017 remained functional at or near 100% throughout the deployment.

No data from secondary sensors are included in the final data files, except when included in OceanSITES files as secondary data. The OceanSITES data repository can be found here: <http://dods.ndbc.noaa.gov/thredds/catalog/oceansites/DATA/KEO/catalog.html>

The KE017 buoy had secondary air temperature, relative humidity, wind, rain, air pressure, and radiation sensors. The only tertiary sensor deployed was a Rotronic HygroClip attached to the Flex system, measuring air temperature and relative humidity. These tertiary data were not distributed in any format.

#### 3.2.1 Winds

TFlex realtime wind transmissions became intermittent October 18, 2019, just prior to typhoon Bualoi. The sensor briefly came back online in late October, but no data was reported thereafter, so the more complete time-series of wind from the Flex system was designated primary. The top plate of the TFlex wind sensor was missing at recovery, and the failure is attributed to the typhoon.

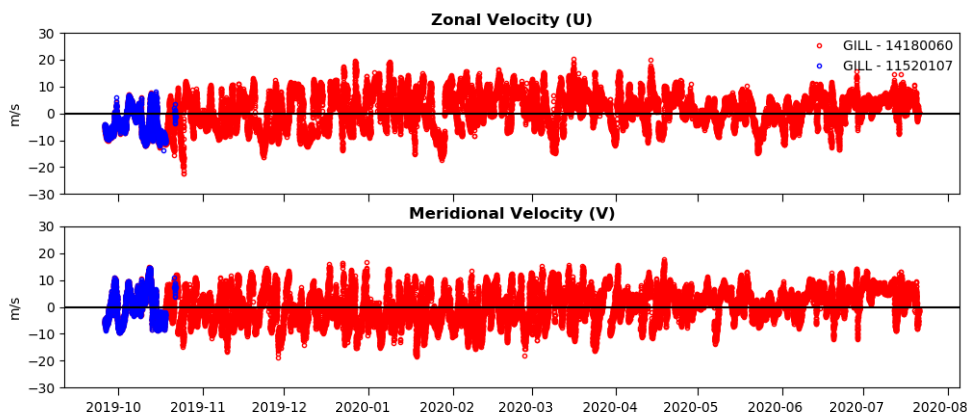


Figure 6: High-resolution wind measurements on KE017.

### 3.2.2 Air Temperature

No issues were experienced in processing KE017 air temperature. All air temperature instruments passed their post-mission calibration procedures, and standard Q2 quality flags were assigned. All three sensors were functional through the end of the deployment.

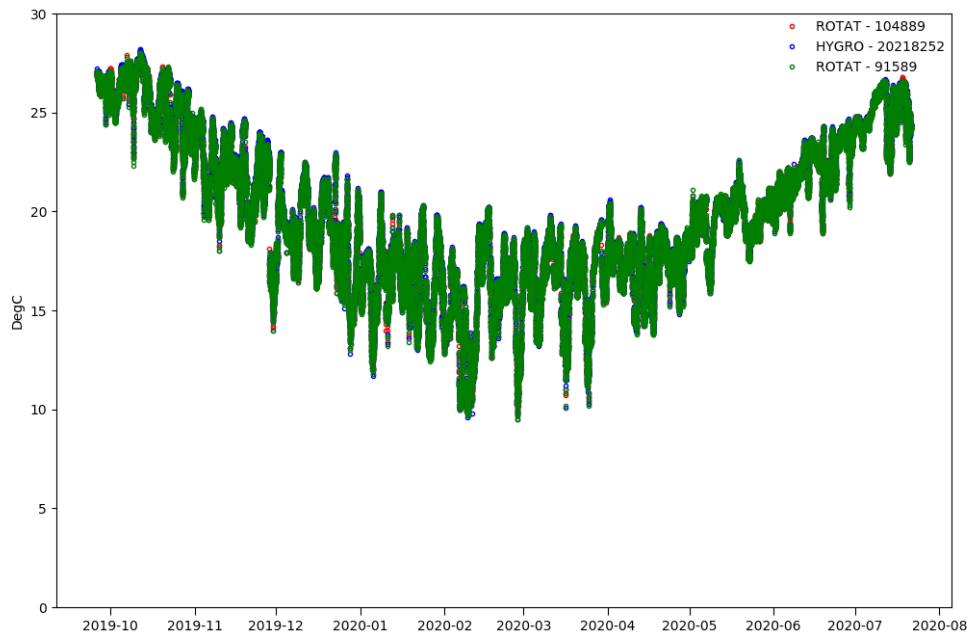


Figure 7: High-resolution air temperature measurements on KE017.

### 3.2.3 Relative Humidity

Both the Flex and TFlex relative humidity sensors on KE017 failed their postcalcs. Noting that the TFlex RH postcal failed with a higher standard error and maximum residual, the Flex sensor remained primary.

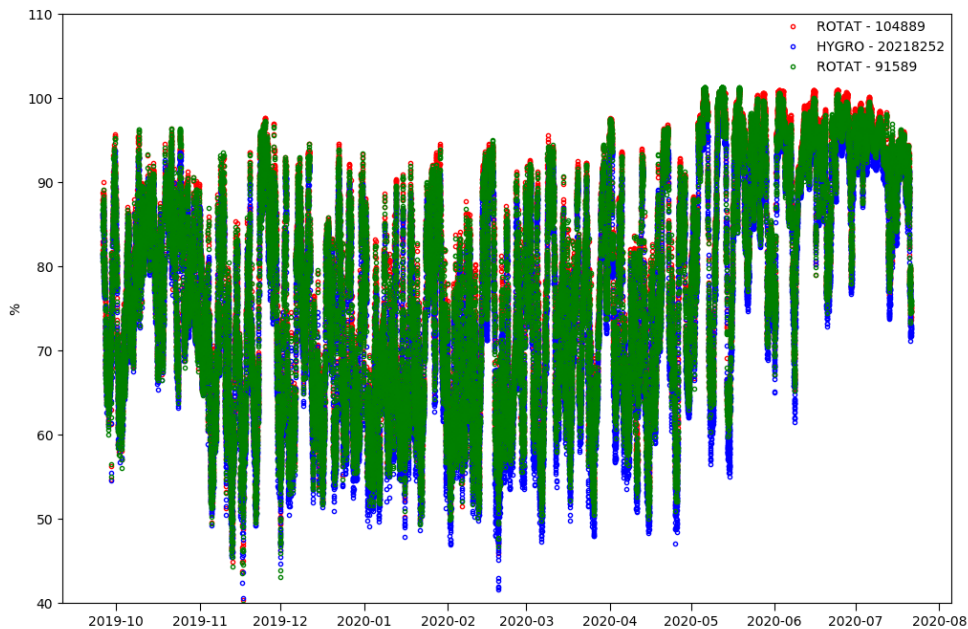


Figure 8: High-resolution relative humidity measurements on KE017.

### 3.2.4 Barometric Pressure

The Flex system's atmospheric pressure was persistently ~0.2mb lower than the TFlex measurement over the course of the deployment, despite agreement to within 0.1mb during pre-cruise testing. Combined with a more consistent handoff from KE016 (not shown), the TFlex data were distributed as primary. As both sensors were the new GE8100 TERPS sensors, improved performance was expected, and both sensors tested well at PMEL. Given the instrument accuracy specification of 0.1mb and the magnitude of the mean difference, the Flex barometer was flagged as lower quality (Q4).

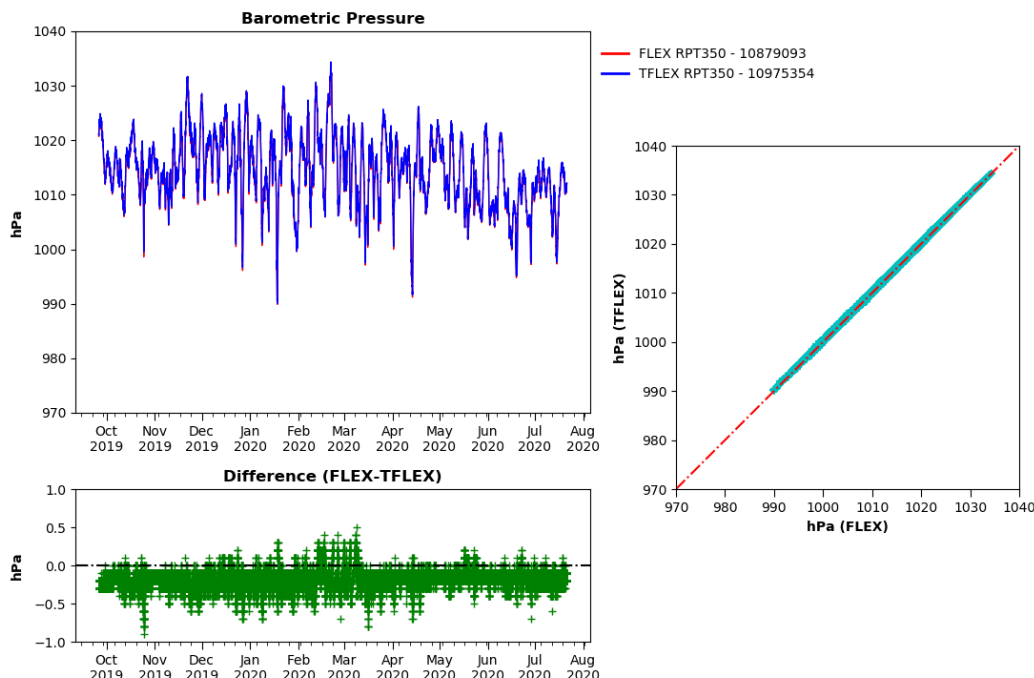


Figure 9: High-resolution barometric pressure data from KE017. The difference plot highlights the persistent low bias of the Flex sensor.

### 3.2.5 Rain

Rain data are acquired as accumulation values, and then converted to rain rates during processing. Rainfall data are collected using an RM Young rain gauge, and recorded internally at a 1-min sample rate. The gauge consists of a 500mL catchment cylinder which, when full, empties automatically via a siphon tube. Data from a three minute period centered near siphon events are ignored. Occasional random spikes in the accumulation data, which typically occur during periods of rapid rain accumulation, or immediately preceding or following siphon events, are eliminated manually.

To reduce instrumental noise, internally recorded 1-minute rain accumulation values are smoothed with a 16-minute Hanning filter upon recovery. These smoothed data are then differenced at 10-minute intervals and converted to rain rates in mm/hr. The resultant rain rate values are centered at times coincident with other 10-minute data (0000, 0010, 0020...).

Residual noise in the filtered data may include occasional false negative rain rates, but these rarely exceed a few mm/hr. No wind correction is applied, as this is expected to be done by the user. The wind effect can be large. According to the Serra, et al. (2001) correction scheme, at wind speeds of 5 m/s the rain rates should be multiplied by a factor of 1.09, while at wind speeds of 10 m/s, the factor is 1.3. As winds are high at KEO, the user is strongly encouraged to apply an appropriate wind correction.

### 3.2.6 Shortwave Radiation

The primary shortwave radiation sensor was chosen based on a system developed by Kelly Balmes during the summer of 2014, using the following criteria:

- Use the sensor with the higher shortwave daily average (if difference is > 1%)
- Use the FLEX system if all else is similar
- Use the sensor that maximizes the time period of available data

Based on these criteria, the KE017 Flex shortwave radiometer was designated primary because the TFlex sensor (S/N 38428) had lower data returns. The TFlex shortwave radiometer was flagged Q5 starting at 10/27/2019 15:57 UTC, the date where nighttime values lifted off the expected nightly baseline of 0 W/m<sup>2</sup>. In November, daytime data became confined to an unexpectedly tight range (about 0 – 400 W/m<sup>2</sup>), inconsistent with typical seasonal variation. Severe drift continued until failure on 2/17/2020. A broken seal and condensation inside the dome were noted during post-mission inspections.

A few outliers were flagged in the Flex shortwave record, when data spiked to ~1,400 W/m<sup>2</sup> on otherwise cloudy days. Historically, marginally high values have been allowed to pass quality control if corroborated by both instruments and given appropriate context (e.g. sunny and clear days). Without the secondary instrument, and given the isolated nature of the spikes significantly higher than surrounding values, Q5 flags were applied.

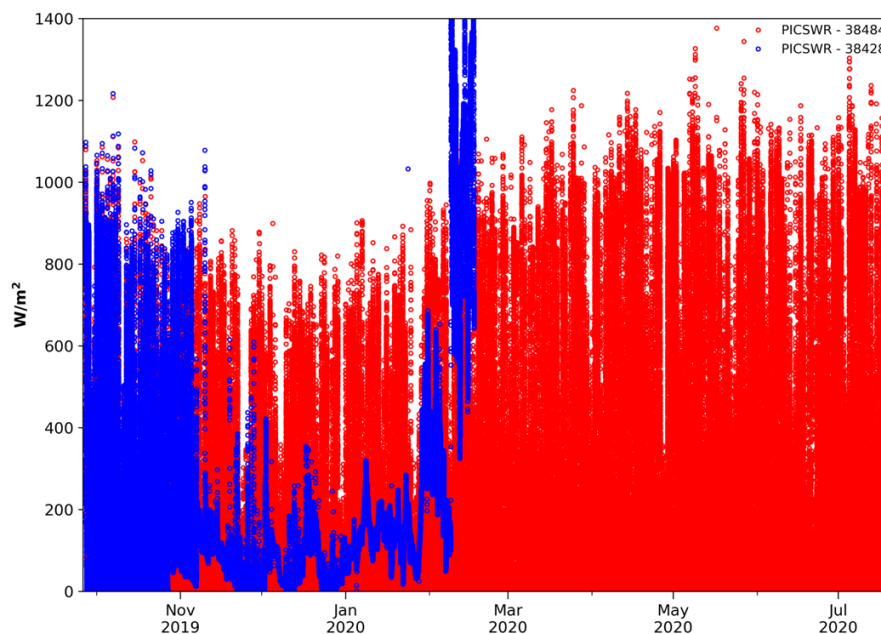


Figure 10: Raw KE017 radiometer data. The TFlex sensor (blue) drifted, then failed.



Shortwave radiation is processed into hourly and daily averaged values differently than other measurements. Because SWR goes to 0 at night, any substantial number of missing values during the night (day) will bias the data high (low). In keeping with GTMBA processing, the percentage of good high-resolution data for SWR must be at least 87.5% in order to generate an hourly or daily averaged data point. Most other instruments use a 50% threshold for high-resolution data needed to generate hourly and daily averages.

### 3.2.7 Longwave Radiation

The downwelling longwave radiation is computed from thermopile voltage, dome temperature, and instrument case temperature measurements, using the method described by Fairall et al. (1998).

Kelly Balmes also developed a set of criteria for determining the primary LWR sensor:

- Use the LWR data from the sensor on the data system that was chosen for SWR
- If LWR data from the first criteria is not available, use the remaining instrument

These criteria were created to maximize data returns and account for bent radiation masts, which are usually detectable by comparing SWR measurements. Although LWR is much less sensitive to orientation, a bent mast can affect either sensor. Clear sky conditions will have a lower LWR than clouds, which are warm due to water content (high LWR). With one LWR and one SWR sensor mounted to each mast, the goal of the criteria is to obtain data from the most vertical mast to avoid a mean tilt when samples are averaged over 1 minute.

Since the KE017 Flex SWR was selected as primary, the Flex LWR would typically be selected as primary under the first criterion. However, the Flex LWR showed signs of drift in both the net LWR and downwelling LWR, so the TFlex sensor was designated primary. Neither mast appeared bent upon recovery.

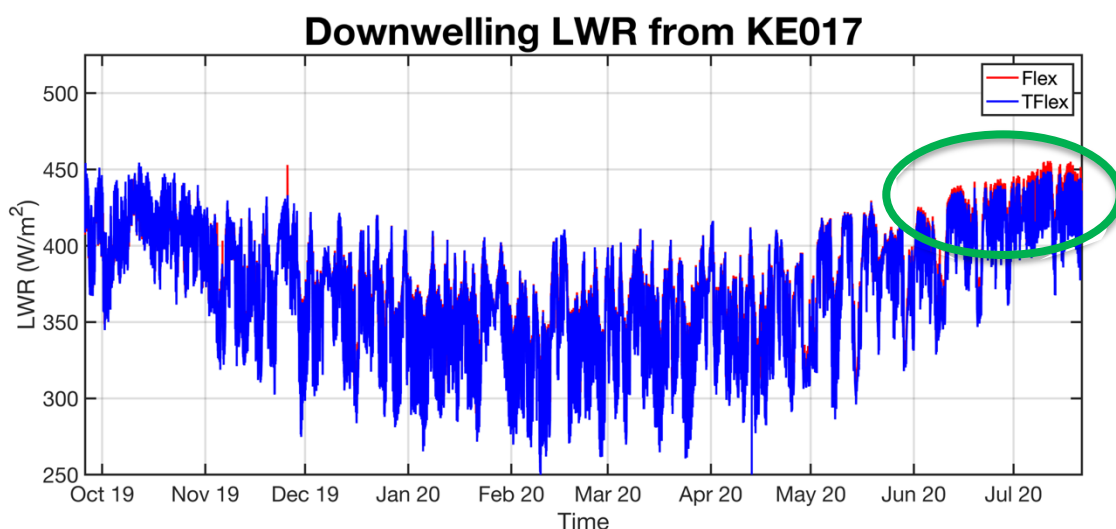


Figure 11: Downwelling LWR (pre-QC) showing spikes, but also data drift ( $>5 \text{ W/m}^2$ , green circle) by the end of the record.

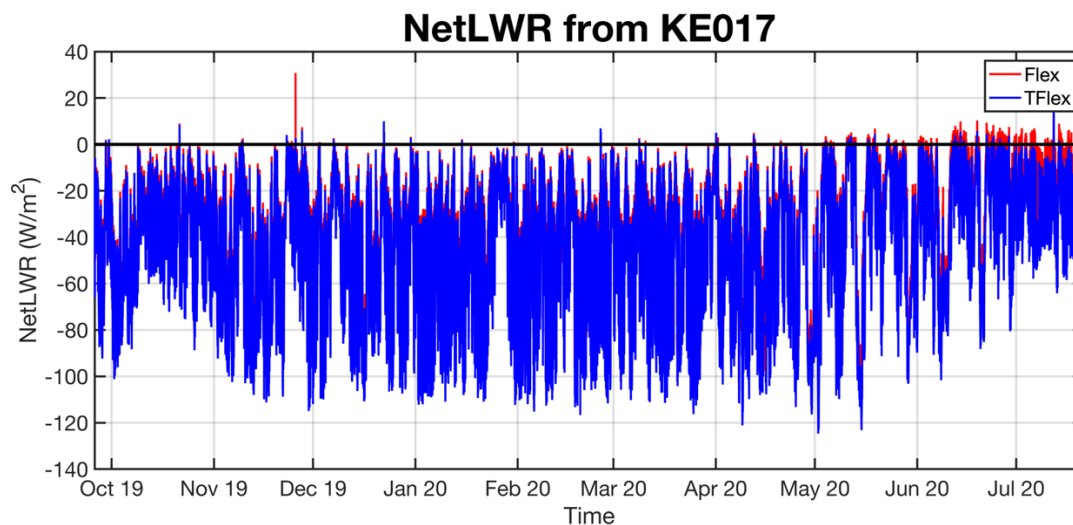


Figure 12: Net longwave radiation (pre-QC) on KE017 showing spikes, but also drift later in the record.

As in other years, thresholds were applied to the LWR data to remove points outside of seasonal bounds. Downwelling LWR exceeding  $475 \text{ W/m}^2$  or positive net LWR continued to differentiate between realistic values and those outside seasonal bounds. In the absence of an inversion, net LWR should not exceed  $0 \text{ W/m}^2$ , which would indicate heat transfer from the atmosphere to the ocean, which is unlikely in the summer.

In the longwave difference plot below (Figure 13), a regime shift is seen around 11/29/2019, after which the range of the differences roughly doubles. With the buoy adrift and no subsequent deployment, no buoy intercomparisons were possible. However, the Flex net LWR was frequently negative in the latter third of the record, so the Flex data quality was lowered (Q4) and the TFlex LWR was distributed as primary.

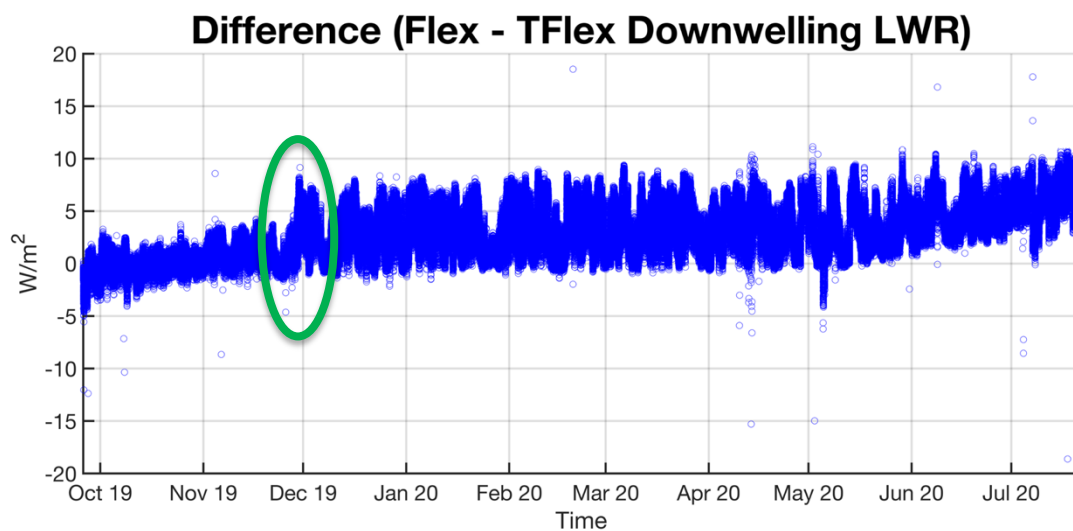


Figure 13: Difference plot of raw (pre-QC) downwelling LWR, showing slow drift, a stepwise separation (circled), and more prominent drift at the end of the record, when the buoy was no longer moored.

### 3.3 Subsurface Data

OCS KEO moorings are instrumented from the surface down to 525m, with one or more deep T/S instruments attached to the acoustic release or other locations near the seafloor. Redundant sea surface temperature and conductivity (SSTC) instruments are deployed on the bridle, which are wired to the Flex and TFlex systems, respectively.

All remaining subsurface instrumentation was connected inductively to the Flex system, except for the instrument attached to the acoustic release and the ocean current profiler. Clock errors from each recovered subsurface instrument are summarized in Table 4. Since no clock errors exceeded half the sampling interval, measurements were mapped to the nearest 10-minute time increment.

The instrument at 475m (S/N 4358) did not report a clock error. Typically, a battery swap will allow for the recovery of any data recorded while the instrument was functioning, and clock errors can be assessed if the battery is not completely depleted. However, no internal time was present, and the instrument reported a sample number of 0, indicating no data records existed.

Type	Serial	Real Time	Inst Time	Clock Error
SBE37-TC-SMP	11554	16:29:35	16:29:32	-0:00:03
SBE37-TC-SMP	7089	16:39:00	16:39:22	0:00:22
SBE37-TC	20433	15:49:10	15:48:44	-0:00:26
SBE37-TC	6077	23:29:15	23:29:30	0:00:15
SBE37-TC	6078	1:05:00	1:05:00	0:00:00
SBE37-TC	6140	16:21:05	16:21:28	0:00:23
SBE37-TC	6079	16:39:00	16:39:15	0:00:15
SBE37-TCP	16293	1:30:00	1:29:56	-0:00:04
SBE37-TCP	7096	1:45:50	1:46:14	0:00:24
SBE37-TCP	12519	15:36:15	15:36:11	-0:00:04
SBE37-TCP	7785	16:20:00	16:20:23	0:00:23
SBE37-TCP	7102	15:53:00	15:53:36	0:00:36
SBE37-TCP	7100	23:57:40	23:58:10	0:00:30
SBE37-TCP	7099	0:06:40	0:06:54	0:00:14
SBE37-TCP	7098	23:39:50	23:40:00	0:00:10
SBE37-TCP	7097	0:51:50	0:52:12	0:00:22
SBE39-TP-IM	4361	19:37:20	19:38:09	0:00:49
SBE37-TCP	7095	0:30:45	0:31:08	0:00:23
SBE39-TP-IM	4359	19:03:00	19:04:17	0:01:17
SBE37-TCP	7094	0:40:10	0:40:47	0:00:37
SBE39-TP-IM	4358			
SBE37-TCP	7093	0:15:55	0:15:20	-0:00:35

Table 4: Recovery log displaying all instrument clock errors.

### 3.3.1 Temperature

Subsurface temperature instruments were set to 10-minute sampling increments. The data are also provided at hourly and daily resolutions. Temperatures are rarely corrected based on post-calibrations, and there was no evidence of drifting temperature measurements.

### 3.3.2 Pressure

Since this was a slack mooring, none of the sensors can be assumed to have been recording measurements at their nominal depths. Users are reminded that the depths of subsurface sensors must be computed from the observed and interpolated pressures contained in the data files.

Pressure measurements were recorded by most of the subsurface instruments. In processing for salinity, interpolated pressures were used if an instrument's pressure sensor failed. In the case of complete instrument failure, where no temperature or conductivity data exists, interpolated pressures were truncated to the time of failure.

The most notable subsurface pressure issues were at 475m, where no delayed-mode records were available, and 425m, where the instrument was loaded with the incorrect calibration (see full discussion of sensor issues in Section 2.3). The inverse relationship between the 425m time series and the surrounding sensors is immediately apparent in Figure 14, but after the correct calibration was applied in post-processing, the pressure data fit into context with surrounding sensors.

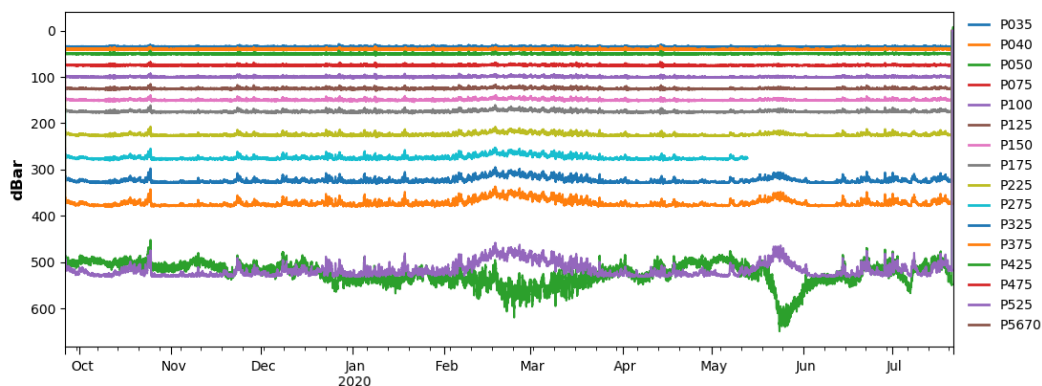


Figure 14: High-resolution subsurface pressure data on KE017 before quality control measures.

### 3.3.3 Salinity

Salinity values were calculated from measured conductivity and temperature data using the method of Fofonoff and Millard (1983). Conductivity values from all depths were adjusted for sensor calibration drift by linearly interpolating over time between values calculated from the pre-deployment calibration coefficients and those derived from the post-deployment calibration coefficients. Salinities were calculated from both the pre and post conductivity values, to determine the drift in the salinity measurement.

Salinity Drifts in PSU (post - pre):

<b>Depth:</b>	<b>Drift:</b>
1m (TFlex)	-0.0308
1m (Flex)	-0.0393
5m	0.0000 **
10m	-0.0083
15m	-0.0144
20m	NaN ***
25m	-0.0070
35m	-0.0257
40m	-0.0269
50m	-0.0239
75m	-0.0435
100m	-0.0310
125m	-0.0282
150m	-0.0264
175m	-0.0166
225m	-0.0174
325m	-0.0146
425m	-0.0044
525m	-0.0151

*\*\* 5m postcal was performed after replatinization, so was not used (high residuals)*

*\*\*\* 20m instrument didn't have a postcal (damaged/failed)*

The values above indicate the change in data values when post-recovery calibrations are applied vs. when pre-deployment calibrations are applied. Negative differences suggest that the instrument drifted towards higher values while deployed, and indicate expansion of the conductivity cell effective cross-sectional area. This expansion is possibly due to scouring of the cell wall by abrasive material in the sea water. Positive values indicate decrease in the cell effective cross-sectional area, presumably due to fouling, and secondarily due to fouling or loss of material on the cell electrodes.

A thirteen point Hanning filter was applied to the high-resolution (ten minute interval) conductivity and temperature data. A filtered value was calculated at any point for which seven of the thirteen input points were available. The missing points were handled by dropping their weights from the calculation, rather than by adjusting the length of the filter. Salinity values were then recalculated from the filtered data.

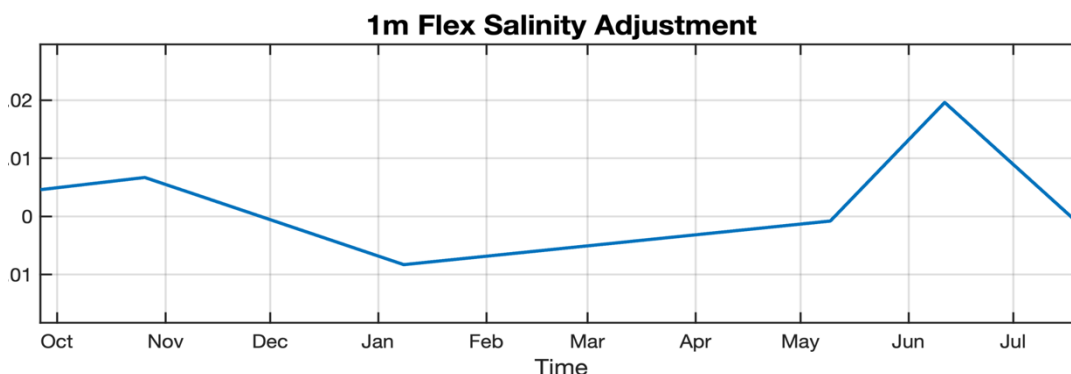
### Manual Salinity Adjustments

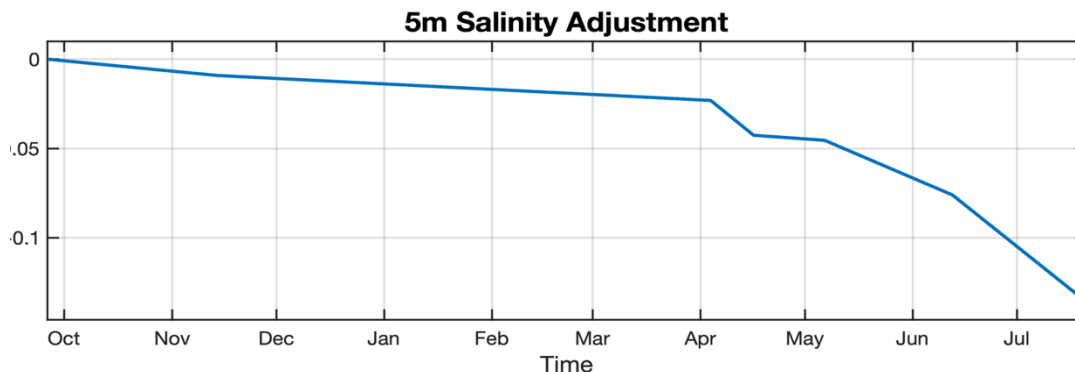
The drift-corrected salinities were checked for continuity across deployments. The range and magnitude of variation matched well with the prior deployment.

Additional linear corrections were also applied to the salinity data in time segments, as noted below. These corrections were based on comparisons with neighboring sensors on the mooring line. If an unrealistic prolonged, unstable density inversion was found, an attempt was made to identify the sensor at fault and adjust its data based on differences with data from adjacent depths during unstratified conditions (e.g. within the mixed layer during nighttime). These *in situ* calibration procedures are described by Freitag et al. (1999).

Based on manual review of the data against neighboring instruments, the following adjustments were made:

2019-09-24 17:44:51 to 2019-11-13 20:48:13 at 5 m adjusted 0.0000 to -0.0091  
 2019-11-13 20:48:13 to 2020-04-03 21:27:43 at 5 m adjusted -0.0091 to -0.0231  
 2020-04-03 21:27:43 to 2020-04-16 06:12:57 at 5 m adjusted -0.0231 to -0.0426  
 2020-04-16 06:12:57 to 2020-05-06 15:27:31 at 5 m adjusted -0.0426 to -0.0454  
 2020-05-06 15:27:31 to 2020-06-12 09:41:59 at 5 m adjusted -0.0454 to -0.0760  
 2020-06-12 09:41:59 to 2020-07-22 12:08:40 at 5 m adjusted -0.0760 to -0.1359  
 2019-09-25 20:27:32 to 2019-10-26 01:31:03 at 1 m adjusted 0.0046 to 0.0067  
 2019-10-26 01:31:03 to 2020-01-08 07:15:02 at 1 m adjusted 0.0067 to -0.0083  
 2020-01-08 07:15:02 to 2020-05-09 13:12:30 at 1 m adjusted -0.0083 to -0.0008  
 2020-05-09 13:12:30 to 2020-06-11 08:05:37 at 1 m adjusted -0.0008 to 0.0196  
 2020-06-11 08:05:37 to 2020-07-21 20:27:32 at 1 m adjusted 0.0196 to -0.0019





A single CTD cast was performed before the KE017 deployment. The cast matched the data well, and was within the expected natural variability of the time-series at each depth.

### 3.3.4 Deep SBE Data

This section of the data report will be updated if and when the two instruments attached to the acoustic release are recovered successfully.

When the KE017 mooring line split, the surface mooring and most of the mooring line went adrift, leaving the anchor, acoustic releases, 2x deep T/S instruments, 18x buoyant glass floats, and a short but unknown length of Polyolefin line as a remnant at depth. After delays due to COVID-19, this mooring remnant was slated for recovery during the 2021 deployment of KE018, but inclement weather prevented a recovery attempt. The next opportunity at recovery will approach the expected 4-year battery life of the acoustic releases. In theory, the acoustic releases will still function past their 4-year battery life, but communication (e.g. triangulation pings or confirmation of release) could be limited.

### 3.3.5 Currents (Nortek Aquadopp)

Upward-looking point current meters were deployed at three depths on the KE016 mooring. The stated head depth differs from the actual current measurement depth, because the instruments require a blanking distance. Currents from the instruments deployed at 8.46, 16.46 and 36.46m measured velocities at 8, 16 and 36m, respectively. The point current meters deployed on KE016 were Nortek Aquadopps.

The current meters calculate the speed of sound, and internally apply sound velocity corrections to current measurements. During post processing, a correction for magnetic declination ( $-5.0^\circ$ ) is applied to the delayed-mode data. A thirteen-point Hanning filter is applied to the 10-minute resolution data to get hourly data, and a boxcar filter produces daily averaged values.

Since the KEO buoy could move about its watch circle, the current meters did not measure true currents. Using time-stamped data from aggregated Flex+TFlex GPS system data, buoy velocity averages were generated. True currents were determined by adding calculated buoy motion to the measured current meter data.

Buoy motion was determined by first interpolating the acquired GPS positions onto a 10-minute grid (:05, :15, :25, etc.). Ten-minute mooring velocities corresponding to the current meter measurement intervals (:00, :10, :20, etc.) were then calculated using the haversine formula, to equate change in position over time to a mooring velocity. The calculated U and V mooring velocities used to correct the current meters are shown in Figure 15.

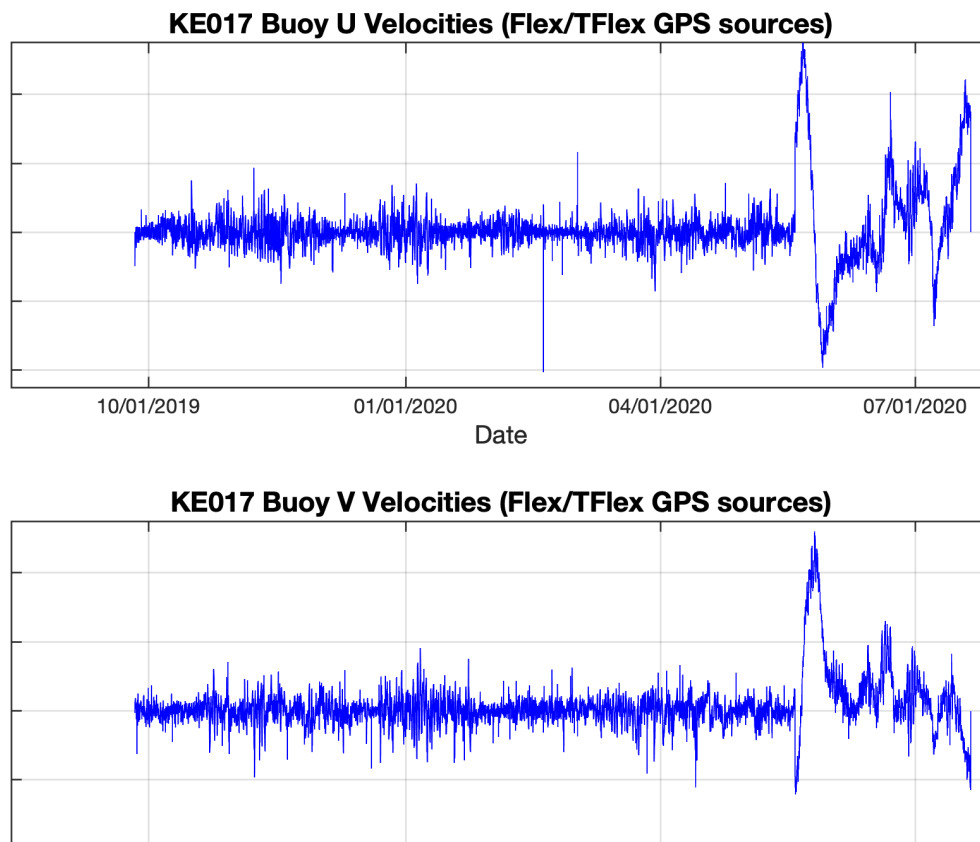


Figure 15: KE017 buoy velocities used to correct currents. The adrift period is apparent in the later part of the record, where buoy velocities starkly deviate from a mean of 0.

No flags were provided by the GPS systems, so data processors flagged the few acquired positions which placed the buoy outside the normal watch circle, but otherwise trusted the reasonable positions and calculated velocities. Note that velocities increase greatly when the buoy breaks free on May 19, 2020. Positions outside the watch circle were eliminated while the buoy was moored, but allowed during the adrift period, during which positions were flagged manually if points were well outside the track of the adrift buoy. A few buoy-motion spikes occur when GPS timestamps are closely spaced, but short periods of high velocities are possible, so positions were not removed.



### 3.3.6 Acoustic Doppler Current Profiler (Aquadopp Profiler)

An upward-looking Aquadopp Profiler was deployed for the second time at KEO, at a depth of 55m. The profiler was downloaded and split into a moored and adrift period (before and after 5/19/2020) for distribution. A snapshot of the profiler data can be found in Figure B5 of the appendix.

To process the data, 4 corrections were applied: declination (-5 degrees), tilt correction, head depth adjustment, and buoy-motion corrections. Aquadopps do not have an internal setting for declination, so this correction to true heading is applied first in post-processing. Tilt correction, also called “bin-mapping,” is then computed using a conversion between Earth and Beam coordinates, taking samples along each beam where it most nearly pierces defined horizontal slices of the water column. Tilts over 20 degrees are eliminated (Q5 flags), as the manufacturer considers data beyond this threshold unusable. A head depth adjustment is needed for the profiler, as its vertical position varies slightly, unlike the previously deployed downward-looking Sentinel ADCP. The data are then regridded using linear interpolation, and buoy-motion is added to U/V currents.

## 4.0 References

Freitag, H.P., M.E. McCarty, C. Nosse, R. Lukas, M.J. McPhaden, and M.F. Cronin, 1999: COARE Seacat data: Calibrations and quality control procedures. NOAA Tech. Memo. ERL PMEL-115, 89 pp.

Fairall, C.W., P.O.G. Persson, E.F. Bradley, R.E. Payne, and S.P. Anderson, 1998: A new look at calibration and use of Eppley Precision Infrared Radiometers. Part I: Theory and Application. J. Atmos. Ocean. Tech., 15, 1229-1242.

Fofonoff, P., and R. C. Millard Jr., 1983: Algorithms for computation of fundamental properties of seawater, Tech. Pap. Mar. Sci., 44, 53 pp., Unesco, Paris.

Serra, Y.L., P.A'Hearn, H.P. Freitag, and M.J. McPhaden, 2001: ATLAS self-siphoning rain gauge error estimates. J. Atmos. Ocean. Tech., 18, 1989-2002.

## 5.0 Acknowledgements

N. Anderson (UW CICOES) processed the Flex/TFlex data. D. Dougherty (UW CICOES) is recognized for designing and generating the initial python files from which processing begins, and for the quality control of real-time data. D. McClurg (UW CICOES) is acknowledged for creating, developing and maintaining the OCS display and delivery pages.

The OCS project office is grateful to the captain and crew of the M/V KAIYO MARU #1, who made the deployment and recovery operations possible. P. Berk, W. Higley, and N. Anderson (all of UW CICOES) participated in the KE017 deployment cruise, and enormous thanks are extended to the captain and crew of the KAIYO MARU #1, who performed a solo recovery of the adrift buoy on July 20, 2020. Covid restrictions prevented a KEO redeployment (KE018), but OCS anticipates the continuation of the KEO timeseries when international business travel resumes.

This work was supported by NOAA's Global Ocean Monitoring and Observing Program (FundRef number 100018302).

## 6.0 Contact Information

For more information about this mooring and data set, please contact:

Dr. Meghan Cronin  
[meghan.f.cronin@noaa.gov](mailto:meghan.f.cronin@noaa.gov)

NOAA/PMEL/OCS  
7600 Sand Point Way NE  
Seattle, WA 98115

## APPENDIX A: Description of Data Quality Flags

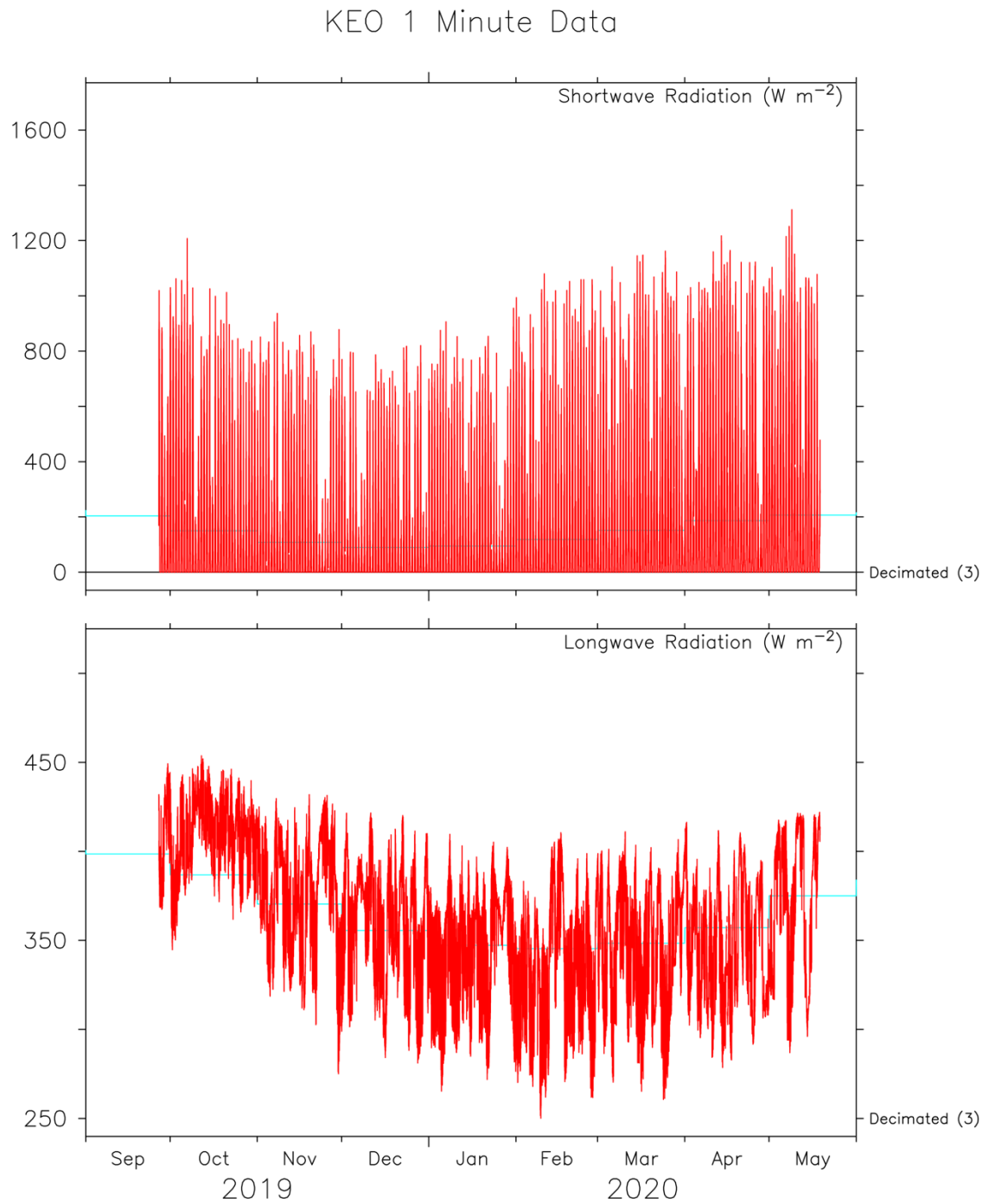
Instrumentation recovered in working condition is returned to PMEL for post-recovery calibration before being reused on future deployments. The resultant calibration coefficients are compared to the pre-deployment coefficients, and measurements are assigned quality indices based on drift, using the following criteria:

- Q0 - No Sensor, or Datum Missing.
- Q1 - Highest Quality. Pre/post-deployment calibrations agree to within sensor specifications. In most cases, only pre-deployment calibrations have been applied.
- Q2 - Default Quality. Pre-deployment calibrations only or post-recovery calibrations only applied. Default value for sensors presently deployed and for sensors which were not recovered or not calibratable when recovered, or for which pre-deployment calibrations have been determined to be invalid.
- Q3 - Adjusted Data. Pre/post calibrations differ, or original data do not agree with other data sources (e.g., other in situ data or climatology), or original data are noisy. Data have been adjusted in an attempt to reduce the error.
- Q4 - Lower Quality. Pre/post calibrations differ, or data do not agree with other data sources (e.g., other in situ data or climatology), or data are noisy. Data could not be confidently adjusted to correct for error.
- Q5 - Sensor, Instrument or Data System Failed.

For data provided in OceanSITES format, the standard GTMBA quality flags described above are mapped to the different OceanSITES quality flags shown below:

- Q0 - No QC Performed.
- Q1 - Good Data. (GTMBA Q1, Q2)
- Q2 - Probably Good Data. (GTMBA Q3, Q4)
- Q3 - Bad Data that are Potentially Correctable.
- Q4 - Bad Data. (GTMBA Q5)
- Q5 - Value Changed.
- Q6 - Not Used.
- Q7 - Nominal Value.
- Q8 - Interpolated Value.
- Q9 - Missing Value. (GTMBA Q0)

## APPENDIX B: Primary Instrument High Resolution Data Plots

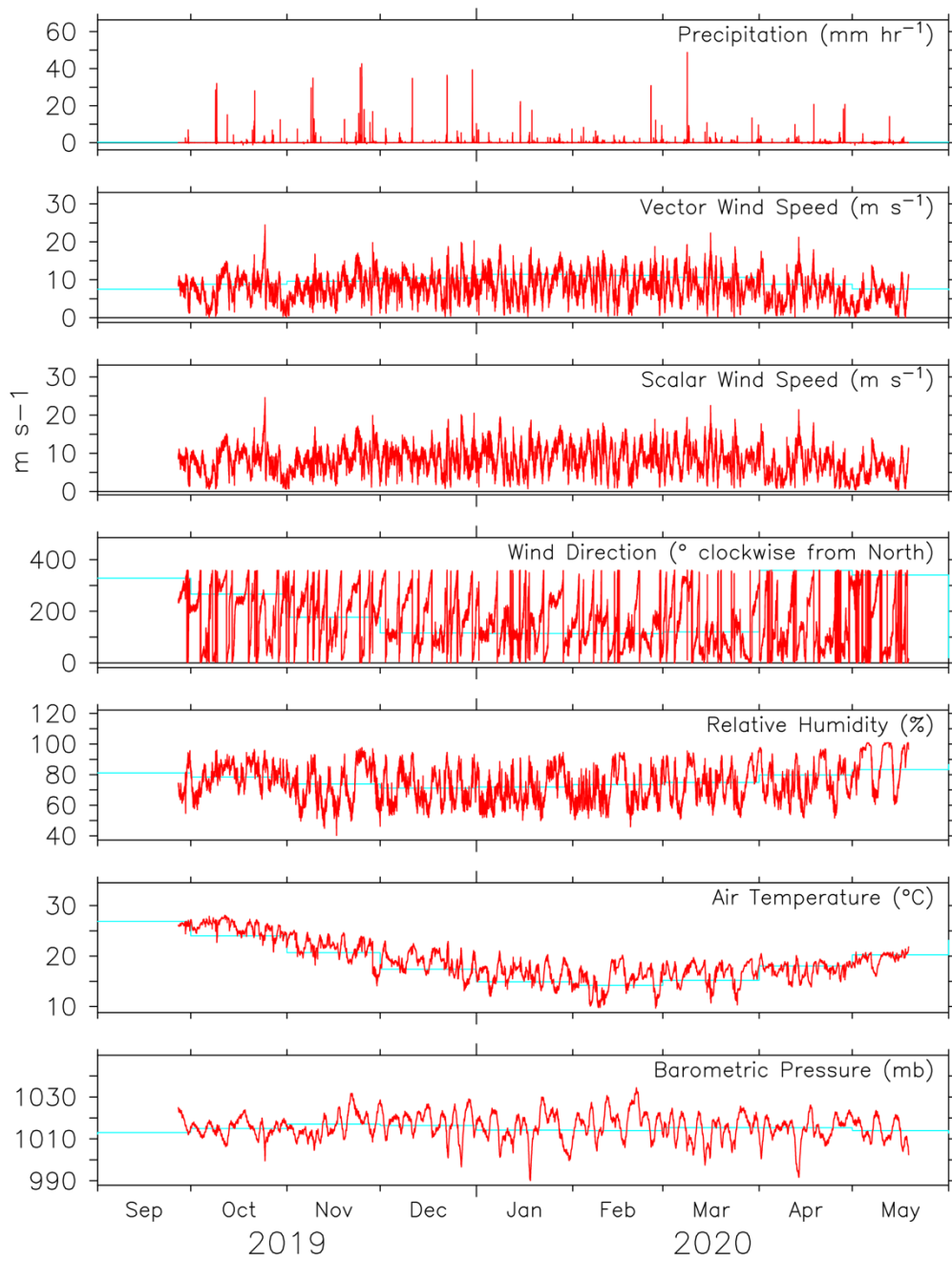


OCS Project Office/PMEL/NOAA

Mar 14 2022

**Figure B 1: KE017 primary shortwave (Flex) and longwave (TFlex) radiation data at 1-min resolution.**

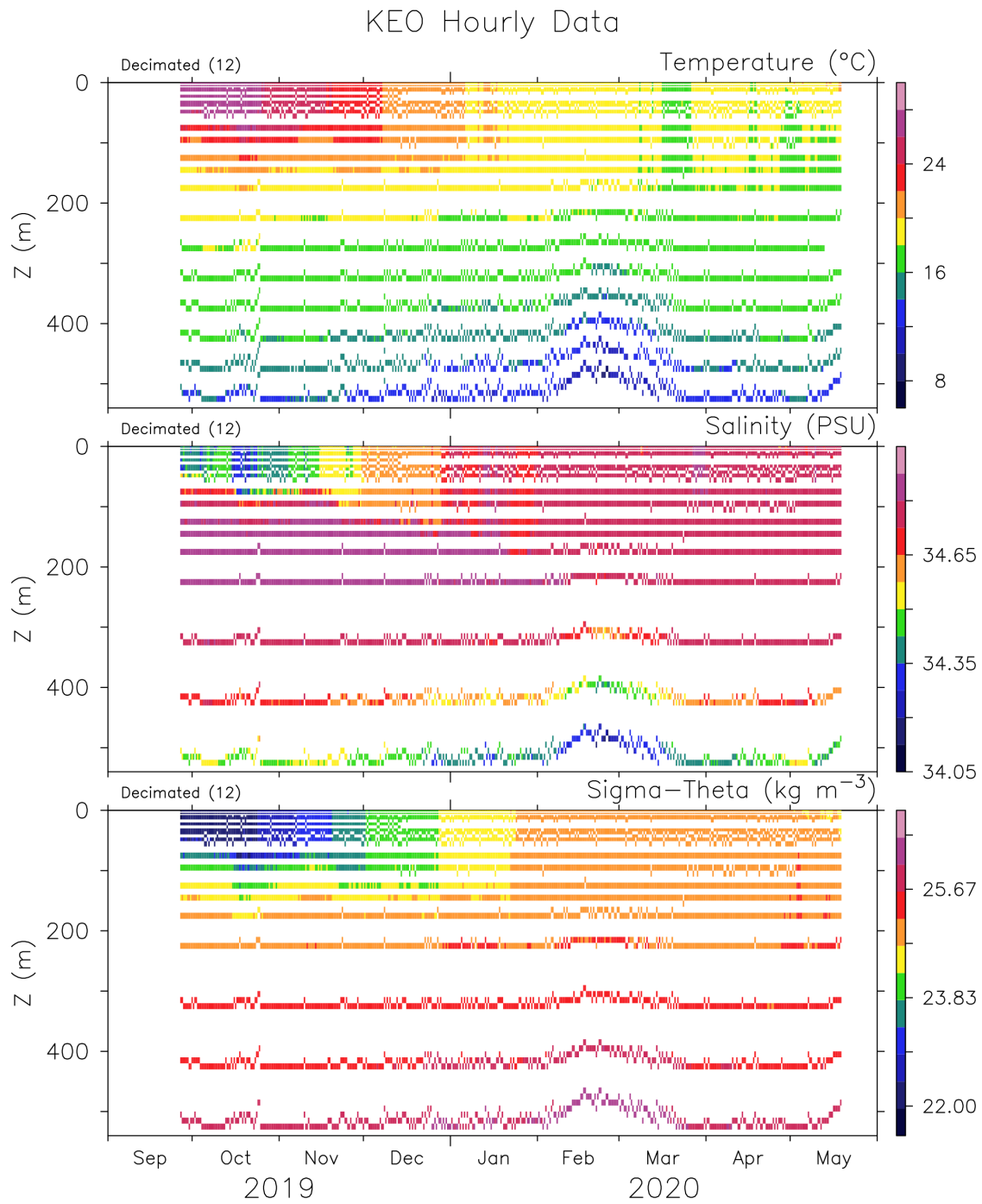
## KEO 10 Minute Data



OCS Project Office/PMEL/NOAA

Mar 14 2022

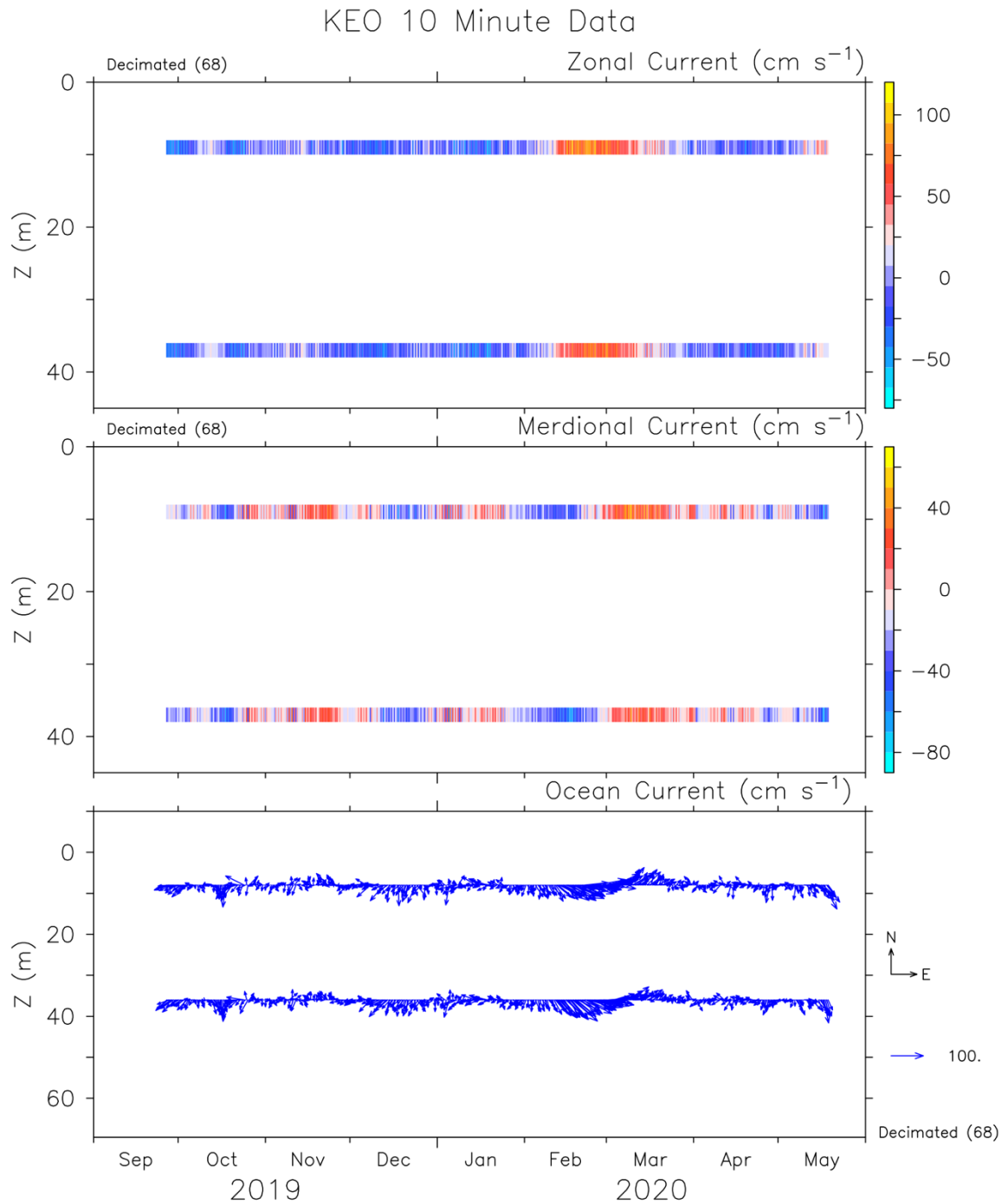
**Figure B 2: KE017 primary meteorological data at 10-min resolution. All data are from Flex, except BP.**



OCS Project Office/PMEL/NOAA

Mar 14 2022

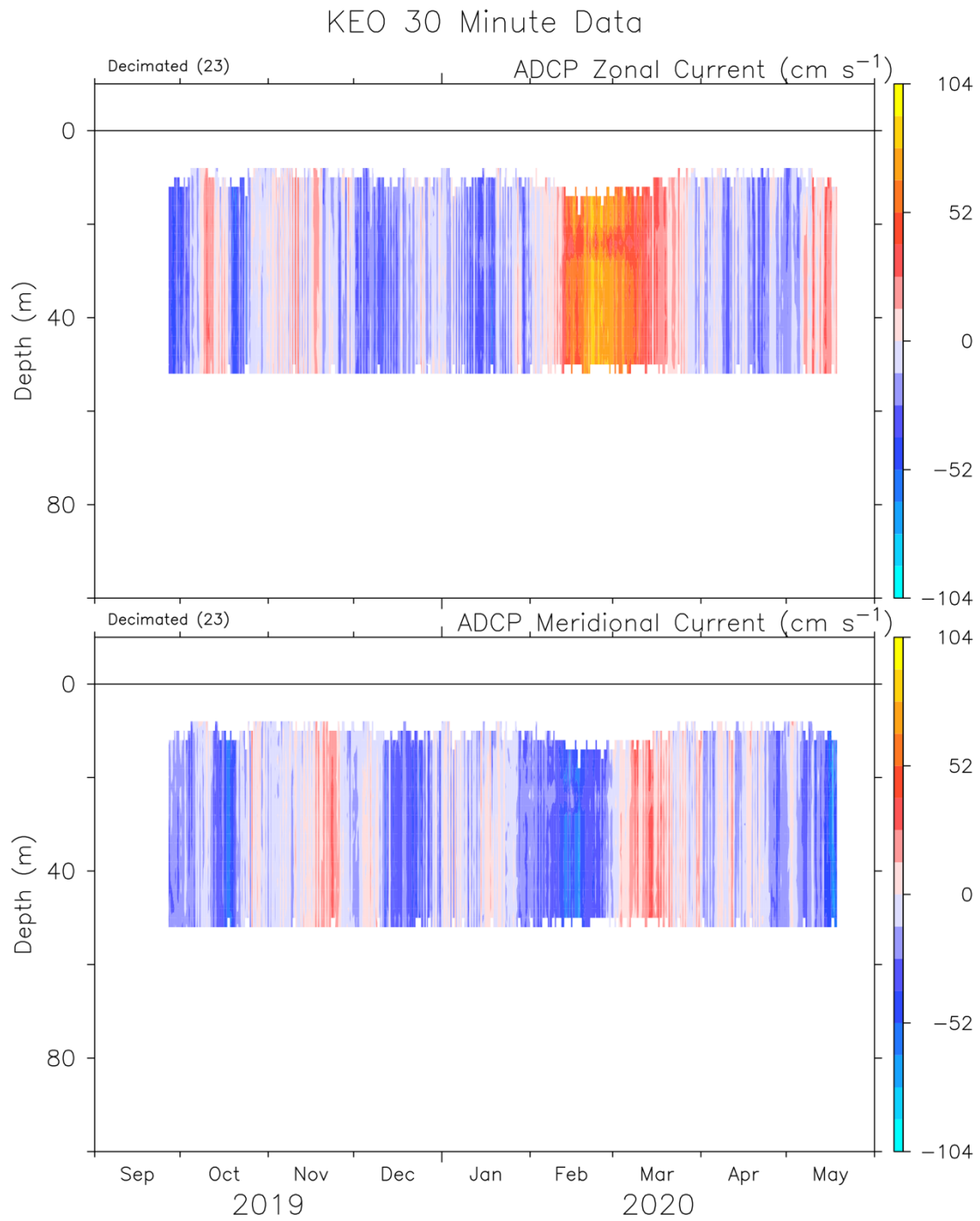
**Figure B 3: KEO17 subsurface temperature, salinity, and density at hourly resolution (decimated).**



OCS Project Office/PMEL/NOAA

Jan 20 2023

**Figure B 4: Zonal and meridional current meter data (decimated) from KE017. Note that 16m realtime Aquadopp data are available (hourly/daily resolution), but the instrument failed to download upon return to PMEL.**



OCS Project Office/PMEL/NOAA

Mar 14 2022

**Figure B 5: Data from the upward-looking Nortek Aquadopp Profiler at 55m. This profiler was deployed for the second time on KE017.**



## APPENDIX C: Secondary Instrument High Resolution Data Plots

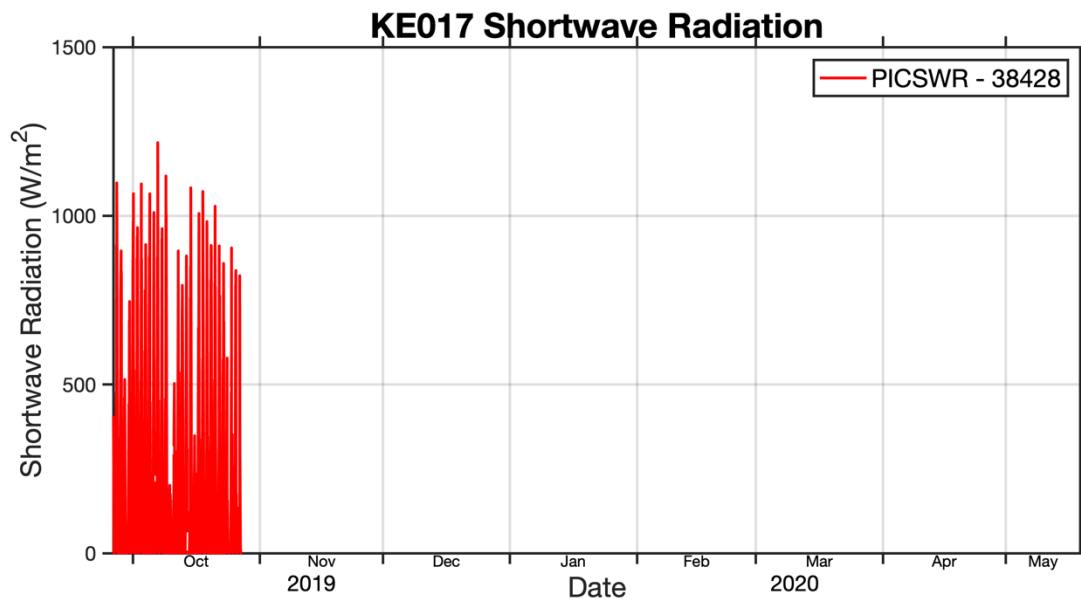


Figure C 1: Secondary (TFlex Eppley PSP) shortwave radiation sensor. The sensor began reporting unrealistic values at night ( $>5\text{W/m}^2$ ) and drifted higher beginning in late October. The remainder of the record was hard-flagged, and the sensor was recovered with a broken seal and visible moisture inside the dome.

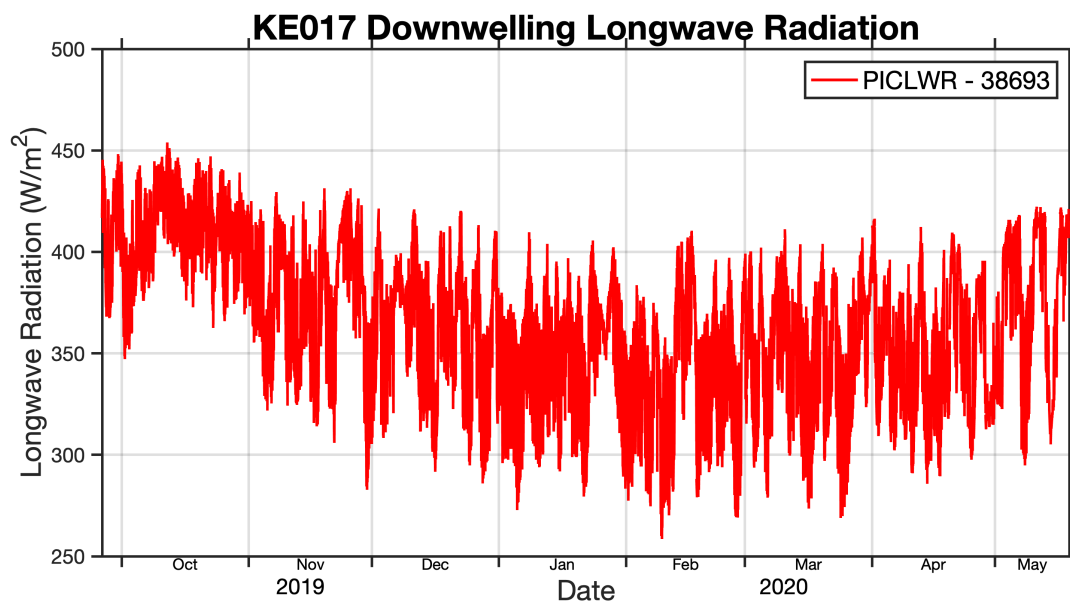


Figure C 2: Secondary (Flex Eppley PIR) longwave radiation sensor.

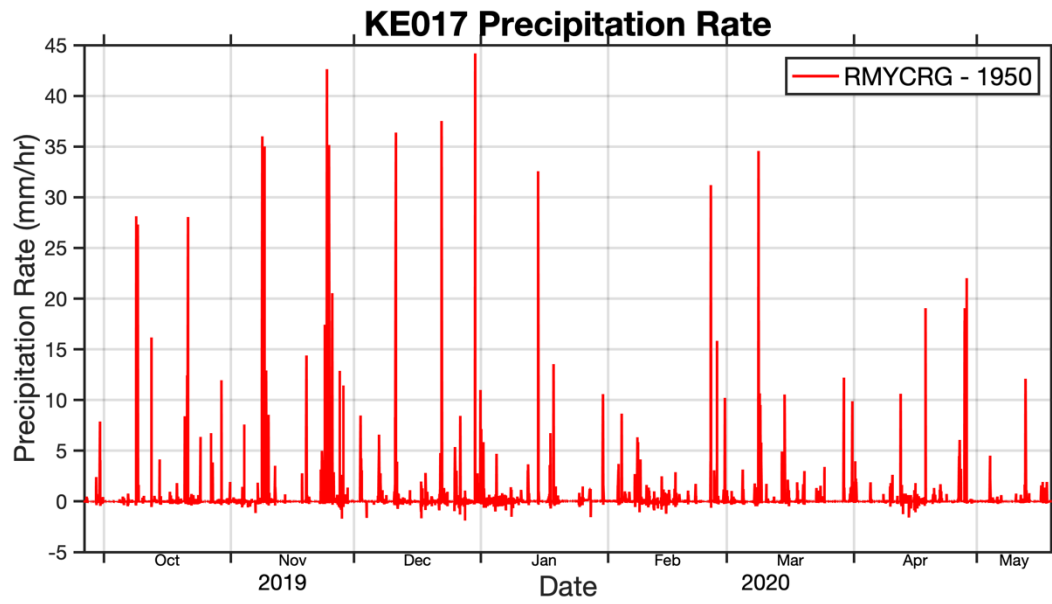
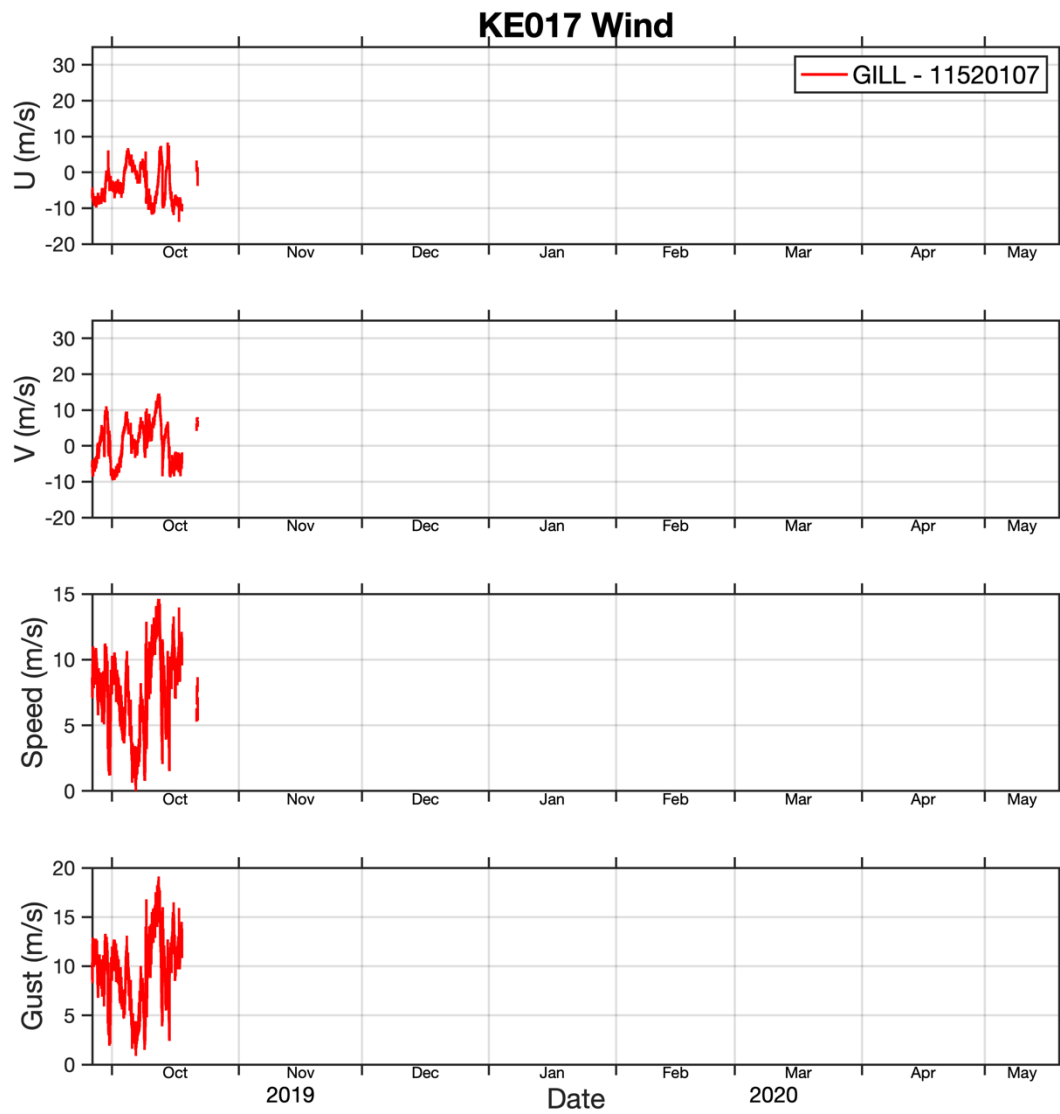


Figure C 3: Secondary (TFlex RM Young) rain sensor.



**Figure C 4: Secondary (TFlex Gill) wind sensor. The top plate of the wind sensor was found missing upon recovery, and the failure is attributed to typhoon Bualoi.**

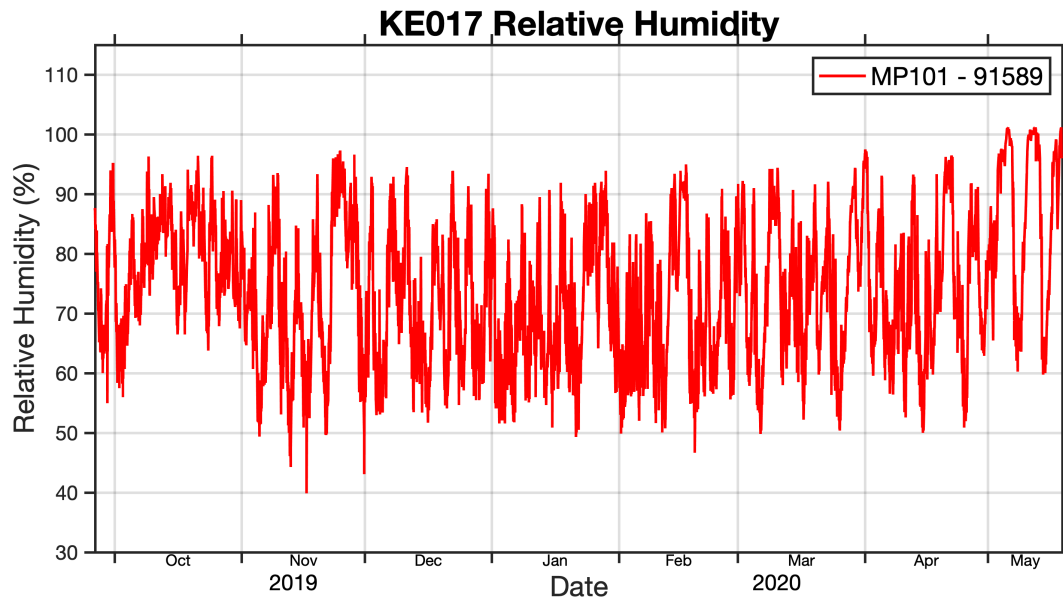


Figure C 5: Secondary (TFlex MP101) relative humidity sensor.

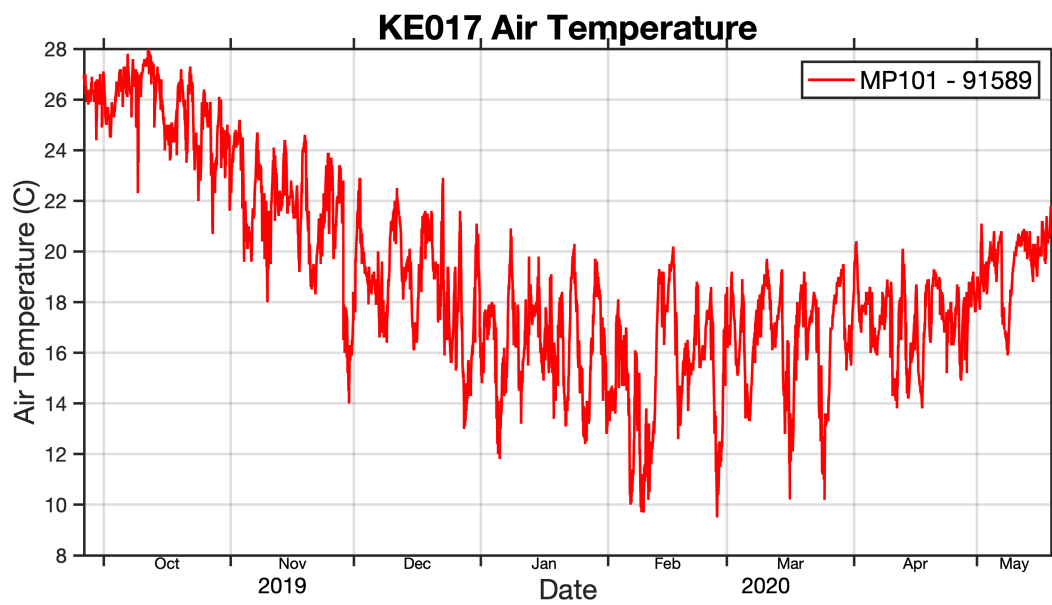


Figure C 6: Secondary (TFlex MP101) air temperature sensor.

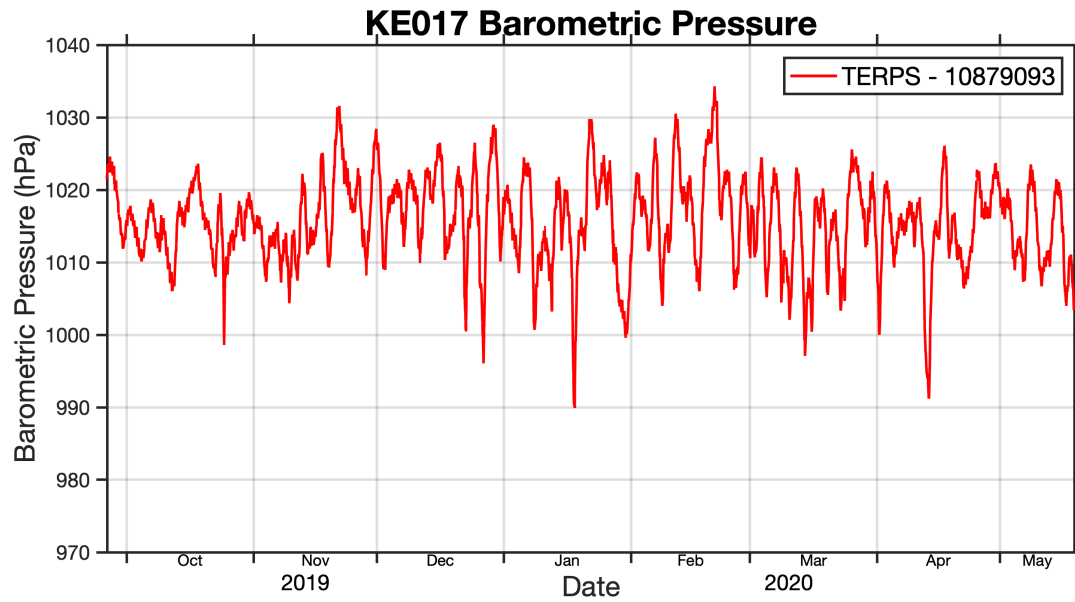


Figure C 7: Secondary (Flex TERPS/GE8100) barometric pressure sensor.

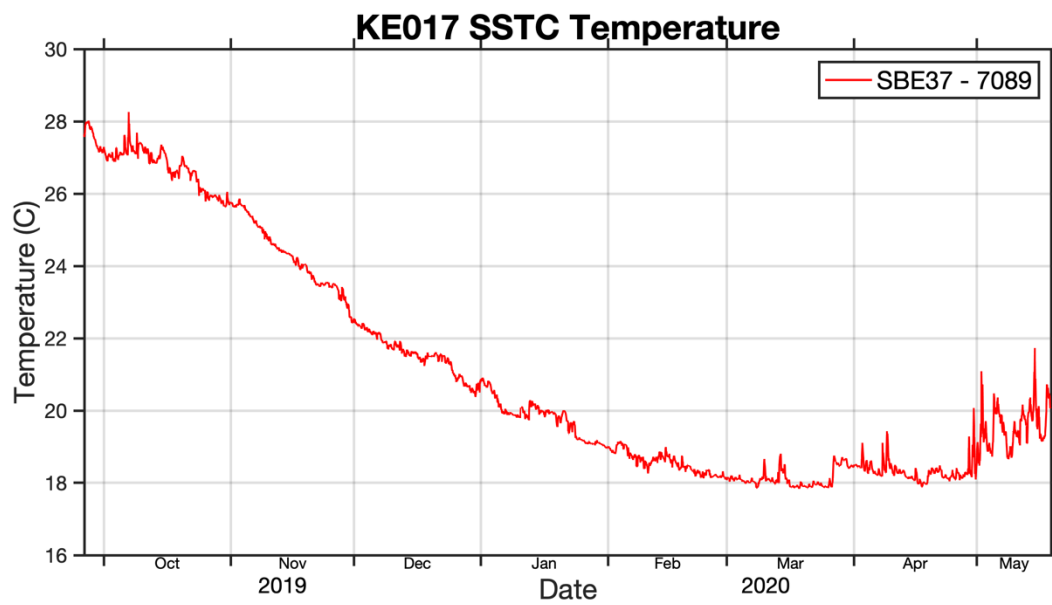


Figure C 8: Secondary (TFlex) SSTC temperature.

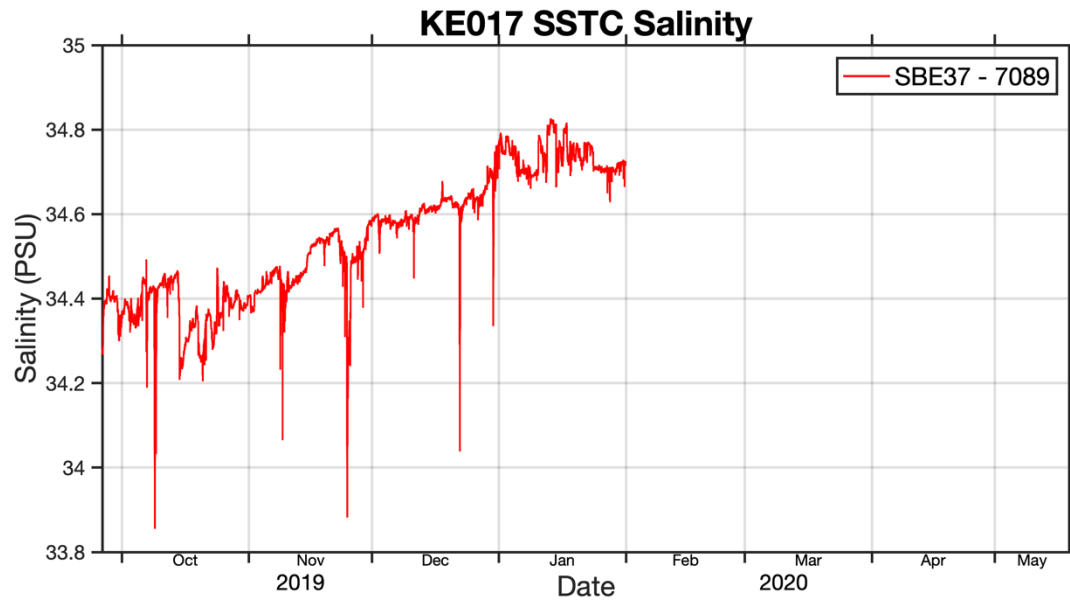


Figure C 9: Secondary (TFlex) SSTC salinity. Records were terminated when excessive noise and spikes down to ~20 PSU began occurring in February.

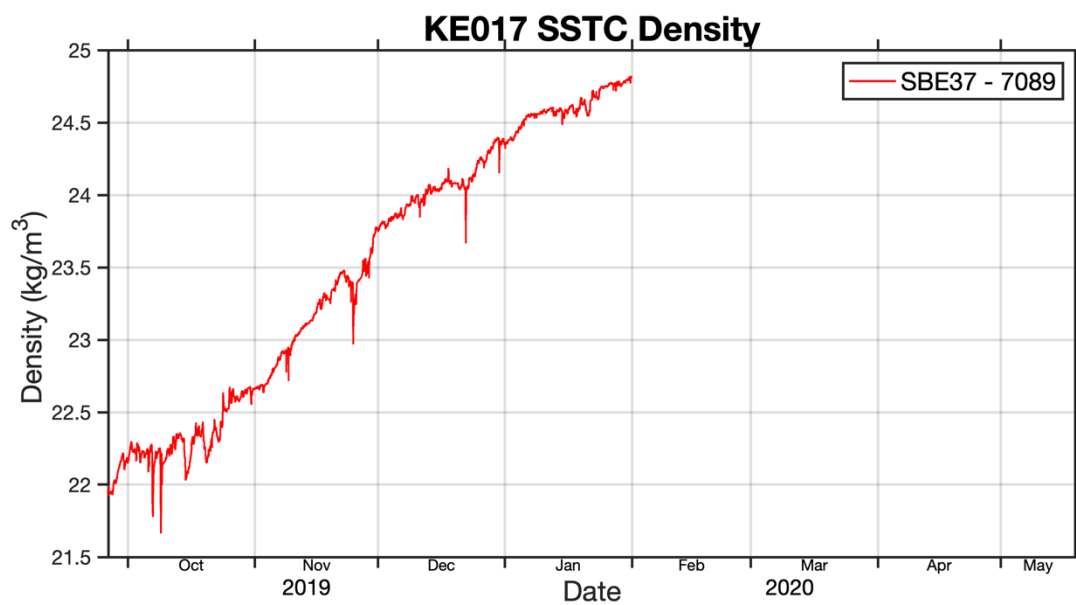


Figure C 10: Secondary (TFlex) SSTC density.